# The Trial of the Holographic Principle

by

Wojciech Musiał

Submitted to the Department of Physics
in partial fulfillment of the requirements for the degree of

Bachelor of Science in Physics and Mathematics

at the

MASSACHUSETTS INSTITUTE OF TECHNOLOGY

June 2013





Author .....
Department of Physics
May 10, 2013

Certified by .....
Allan W. Adams
Assistant Professor
Thesis Supervisor, Department of Physics

Accepted by .....
Nergis Mavalvala
Professor
Senior Thesis Coordinator, Department of Physics

# The Trial of the Holographic Principle

by

Wojciech Musiał

Submitted to the Department of Physics
on May 10, 2013, in partial fulfillment of the
requirements for the degree of
Bachelor of Science in Physics and Mathematics

## Abstract

We present an introduction to ideas related to the holographic principle in the context of the well-established duality between classical gravity and conformal fluid dynamics. Foundations of relativistic hydrodynamics, conformal invariance, and geometry of anti-de Sitter spaces are discussed.

We then detail an explicit calculation relating the dynamics of a non-stationary non-symmetrical $3+1$ dimensional black hole on an anti-de Sitter background to the dynamics of a $2+1$ conformal fluid. The correspondence is established in a perturbative series expansion of the black hole metric, corresponding to a hydrodynamical expansion of the stress-energy tensor of the dual fluid. The stress-energy tensor of the dual fluid, whose conservation arises as a consequence of Einstein field equations of the dual black hole, is calculated via the Brown-York prescription augmented with renormalization of divergences. While the fluid-gravity idea is well-established, our careful analytic computation finds a form of the metric computed at second order in the gradient expansion that differs in some respects from results in previous literature.

We finally report results of our work to realize the fluid-gravity duality numerically. We have solved $2^{\text{nd}}$ order hydrodynamic flow numerically and attempted to construct the black hole metric dual to the flow. Investigation of power law scaling of the Einstein tensor indicates success at $0^{\text{th}}$ and $1^{\text{st}}$, but not the $2^{\text{nd}}$ order. We have also observed in a low-resolution simulation that the hydrodynamic flow supports turbulence, which prompts the question of the interpretation of dual turbulent behavior of the black hole geometry.

Thesis Supervisor: Allan W. Adams
Title: Assistant Professor

## Acknowledgments

I am greatly indebted to Professor Allan Adams for invaluable guidance and shaping of ideas which became the subject of this thesis. His insights opened new venues of thought, ethics of work left a life-long imprint, and undepletable enthusiasm covered up for my mistakes and also bad weather.

I would also like to thank a fellow student and a collaborator Nathan Benjamin for helpful discussions and invaluable endurance in carrying out this research, as well as nameless listeners whose kind receptiveness and encouragement was as important.

# Contents

# Chapter 1

# Introduction

Holographic principle is an idea that applies to physical systems whose $d$-dimensional dynamics can be encoded in an equivalent description of lower dimensionality. Initially motivated by the fact that the black hole temperature grows as the horizon *area* and not volume, the holographic principle has been observed for type IIB superstring theory on a background $AdS_5 \times S^5$ geometry and its dual $SU(N)$ Yang Mills description, which eventually lead to the formulation of the infamous AdS/CFT conjecture [7]. For an excellent recent introduction to the AdS/CFT ideas, see Chapter 4 of [21], as well as [18].

The ideas of holographic duality explored in this paper can be regarded as a finite temperature, low energy case of the AdS/CFT conjecture, as it describes the duality between a conformal relativistic fluid in $2+1$ dimensions and a $AdS_4$ classical gravity. This fluid-gravity duality is a well-established idea with salient results presented in [13], [14], [15], [17], [19], [20], as well as in an excellent pedagogical review [16].

Numerical tests of the fluid-gravity duality have been carried out for various spacetime geometries. In particular, [22] constructed a $2+1$-dimensional $0^{\text{th}}$ order hydrodynamic flow dual on a sphere dual to $AdS_4$, while [23] numerically solved Einstein gravity in $3+1$ AdS and numerically found the stress-energy tensor of the $2+1$-dimensional conformal fluid dual to the geometry. We test the holographic principle in a direction opposite to [23]: we construct the geometry of a dynamical, out-of-equilibrium $AdS_4$ black hole by solving the $2+1$-dimensional conformal fluid equations. The numerical results indicate success at order 0 and 1 in the long-wavelength perturbation expansion. Order 2 results are problematic: investigation of the Einstein tensor for the $2^{\text{nd}}$ order metric constructed out of the simulated hydrodynamical flow shows inconsistencies. We believe the issue is entirely due to a bug in the numerical code, which we will subject to a more scrutinous analysis in the future.

Additionally, we carry out an investigation of turbulence similar to [22] and verify that the $2^{\text{nd}}$ order $2+1$-dimensional relativistic conformal fluid on a torus exhibits turbulent behavior at appropriate dissipation scales.

This paper is organized as follows. In Chapter 2 we provide a pedagogical review of basic ideas of relativistic hydrodynamics. In Chapter 3 we discuss briefly the geometry of anti-de

Sitter space-times, as well as the construction of the Brown-York boundary stress energy tensor. Chapter 4 is concerned with the fluid-gravity duality. We first outline carefully the fluid-gravity perturbative analysis pioneered in [13] and specialized to $2+1$-dimensional fluid in [14]. We then present results of our analytical calculations, which are found to differ in some respects from [14]. Lastly, we present and discuss results of our numerical simulations.

# Chapter 2

# Hydrodynamics

In this section we present a brief introduction to the theory of fluid dynamics, its relativistic generalization and introduce mathematical machinery relevant to the study of the fluid-gravity correspondence.

The theory of fluid dynamics is concerned with describing a classical macroscopic behavior of a microscopic system [2]. Since all known physical systems are believed to comprise of a large numbers of degrees of freedom that are quantum in nature, hydrodynamics is necessarily as an *effective* low energy, long wavelength description of some microscopic system. As our everyday experience with systems of many degrees of freedom confirms, dynamics at macroscopic scales is continuous despite the possibly discrete or quantum nature of the microscopic scale. Hydrodynamics averages over the many "ridges" of discrete degrees of freedom and describes them in terms of few continuous macroscopic variables such as mass density $\rho$, pressure $p$ and derivatives thereof. As an example, the net aggregate motion of the microscopic degrees of freedom is encoded by a smooth velocity field. The macroscopic variables, despite varying in space and time, should be thought of as thermodynamical: fluid elements at every point in space and time are assumed to be in local equilibria, and as such are described by a set of thermodynamical variables, which themselves must also vary from point to point.

As a result of the kinematics of and interaction between individual microscopic degrees of freedom, the hydrodynamical variables change in time: energy and momentum flow from place to place, and the form of energy changes between kinetic and potential. To account for the dynamics, one must therefore supplement the fluid variables with a set of local dynamical equations (differential equations in the time variable). It is not immediately clear that this can always be done. If the microscopic degrees of freedom are interacting, then the field equations for their effective hydrodynamical behavior are necessarily non-linear. If, in addition, we allow for the inclusion of arbitrary powers of derivatives in the dynamical equation, there is an infinite number of possible terms one could write down! The difficulty of uniqueness and convergence is resolved by introducing a hierarchy of orders on the derivatives of the hydrodynamical variables—higher-order derivatives become less

and less important—and truncating the description at a given order. Assertion of this hierarchy, known as the *hydrodynamical assumption* is in fact equivalent to the assumption of local equilibrium: no fluid whose high-order velocity gradients do not become small can be regarded as locally well-behaved, and vice versa.

## 2.1 Relativistic stress-energy tensor

We now turn our attention to the formulation of a relativistic hydrodynamical theory, with the goal of arriving at fully relativistic equations of motion. One could in principle invent the equations of motion bottom-up by writing down a dynamical equation in time consistent with the requirements of special relativity, but that is a crude approach: the symmetries of the system may not be manifest, and the form of physical observables obscured. Instead, we observe that equations of motion must conserve energy and momentum and proceed to obtain the equations of motion as appropriate conservation equations.

In order to describe the flow of energy and momentum in a continuous medium, we need a tensorial quantity that encapsulates the information of stresses, densities, and momenta at every point in space. For this reason, a simple relativistic four-momentum is insufficient. The conservation equations $\partial_\mu p^\mu$ do not account for flow of potential energy in space. Motivated by classical fluid mechanics, we define the relativistic *stress-energy tensor* $T^{\mu\nu}$ as a generalization of the non-relativistic stress tensor, in the following sense. The components of a non-relativistic stress tensor give us forces across surfaces of infinitesimal fluid element, which we can also think of as time fluxes of momentum in a direction perpendicular to spacelike surfaces. To make a leap to a relativistic generalization, we notice that what a Newtonian physicist calls a "flux in time" is really a density along a timelike direction to a special relativist. We thus define the components of $T_{\mu\nu}$ as the natural relativistic generalization (inspired by the discussion in [1]):

$$T^{\mu\nu} = \text{density four-momentum } p^\mu \text{ across the 3-surface orthogonal to the direction } \nu. \tag{2.1}$$

Despite dubious looks, the resulting object is in fact a proper Lorentz rank two tensor – one can think of $T^{\mu\nu}$ as $\lim \Delta p^\mu / \Delta \mathrm{Vol}_3$ and observe that a 3-volume element perpendicular to a four-direction is a dual one-form, and hence transforms as a genuine rank-1 tensor.

In the non-relativistic limit, the space components of $T^{\mu\nu}$ reduce to the classical stress tensor: the flux of the space components four-momentum across the 3-surface orthogonal to a spacelike direction is the *time* flux of momentum in space. The time components are more interesting: $T^{00}$, the "flow" of energy across spacelike surface is just the energy density, while $T^{0i}$ is a measure of the density of spatial momentum. To build Lorentz covariant quantities with a physical meaning we note that in a frame of reference where the local fluid element is at rest, we can extract the "0" components by contraction with

the fluid velocity $u = (1, 0, 0, \dots)$. The rest frame energy density $\rho$ is therefore a Lorentz scalar:

$$\rho = T^{00}{}_{\text{rest}} = T^{\mu\nu} u_\mu u_\nu \tag{2.2}$$

while the the momentum density—a Lorentz vector—depends on the observer's frame:

$$p^\mu = T^{0\mu} \tag{2.3}$$

We are now in a position to impose conservation of energy-momentum in a usual way by demanding that the divergence of the density of four momentum vanishes:

$$\partial_\mu T^{\mu\nu} = 0 \tag{2.4}$$

To see that this is indeed the appropriate conservation equation, we check that it indeed is necessary for the conservation of momentum. To this end, we compute the time change in the total momentum $P^\mu = \int \mathrm{d}x^n\, p^\mu$ as seen is the observer's frame of reference:

$$\frac{\mathrm{d}}{\mathrm{d}t} P^\mu = \int \mathrm{d}x^n\, \partial_t T^{0\mu} = -\int \mathrm{d}x^n\, \partial_i T^{i\mu} = 0 \tag{2.5}$$

where the second equality sign follows by eq. (2.4), and the third is zero by the divergence theorem.

The hydrodynamics assumption—diminishing in size of subsequent derivatives of the hydrodynamical variables—allows us to write the stress energy tensor as an "expansion" in the order of spacetime derivatives. The word "expansion" should be approached with caution, for it is not used in the usual sense of a series in a small parameter. Instead, we postulate that the stress-energy tensor can be decomposed into a sum of Lorentz covariant terms built out of fluid velocity and its derivatives, and we classify them by the number of spacetime derivatives. Pictorially, we write this as:

$$T^{\mu\nu} = T_0^{\mu\nu} + T_1^{\mu\nu} + T_2^{\mu\nu} + \cdots \tag{2.6}$$

The hydrodynamics assumption now asserts that the order of the contributions displayed above is in fact the order of diminishing importance. If we were interested in describing a fluid in a long-wavelength regime, we can truncate the series at a desired order with little penalty. Then, terms compatible with symmetries of the theory appearing at any order in the expansion are added together with some coefficients, which could in principle be measured by an experiment.

Often, the spacetime indices appear in equations with no apparent function, such as in the equation (2.6) above. We will suppress them if no confusion arises.

### 2.1.1 Ideal fluid stress-energy tensor

In this section we should shortly see that the description of an ideal (zero viscosity) fluid involves only stress-energy terms at the leading $0^{\text{th}}$ order. Indeed, in a fluid with non-zero viscosity, a moving fluid element encounters resistance. This resistance causes matter, and thus momentum, to disperse (flow) in spatial directions, and the dispersion must depend parametrically on the difference between velocities of the local fluid element and its surroundings, i.e. the derivatives of the fluid velocity. Those effects are absent with zero viscosity, and it is reasonable for us to expect that $T_1 = T_2 = \cdots = 0$.

How do we construct the stress energy tensor then? We need to "measure" the energy information of a fluid element, and there is no better place to do that but in the fluid frame of reference. Since the fluid is completely still, the relativistic energy density is simply the fluid mass density:

$$T^{00}{}_{\text{rest}} = \rho. \tag{2.7}$$

As the ideal fluid experiences no shear stresses nor momentum dissipation, all of the off-diagonal components are zero. The spatial diagonal elements, the time and two-volume densities of spatial momentum (or the time flow of momentum across surfaces), are nothing else but the fluid pressure. In addition, the ideal fluid in its rest frame is isotropic: there is no preferred direction set by the fluid velocity. All of the pressure components must be equal. We therefore conclude:

$$T_{\text{rest}} = \text{diag}\,(\rho,\, p,\, \ldots,\, p) \tag{2.8}$$

A covariant expression for the stress-energy tensor is readily constructed as:

$$T_0^{\mu\nu} = \rho\, u^\mu u^\nu + p\,(\eta^{\mu\nu} + u^\mu u^\nu) \tag{2.9}$$

### 2.1.2 Stress-energy tensor at higher orders

The ideal fluid stress-energy tensor constructed above does not include viscous effects *by design*. So far we observed that the stress-energy tensor can be written as a sum of terms ranked by number of spacetime derivatives, and that dissipative effects can only be captured by terms involving fluid velocities. In order to "correct" the ideal fluid description to capture viscous effects we should therefore incorporate higher-order derivative terms. Before that can be done, it will be of great advantage to classify all valid contributions to $T^{\mu\nu}$ at the leading first and second order.

To begin, we notice that the corrections cannot be arbitrary. $T^{\mu\nu}$ is symmetric, and so must the higher-order pieces $T_i^{\mu\nu}$. Moreover, recall that we *defined* $u$ to stand for the local fluid velocity. This definition forces a general constraint on $T$: contractions with fluid velocities must give the mass density (2.2). Furthermore, in the local frame of the fluid, the four-momentum density must arise entirely due to motion of the fluid mass. The latter

constraint is stronger than the former, and can be concisely written as:

$$T^{\mu\nu}\, u_\mu = \rho\, u^\nu \tag{2.10}$$

Since this constraint is already met by the $0^{\text{th}}$ order ideal fluid, we conclude that all higher-order pieces of $T$ must be $u$-orthogonal:

$$T_i^{\mu\nu}\, u_\mu = 0 \tag{2.11}$$

While it is easy to write down an arbitrary Lorentz-covariant term that involves a given number of derivatives (say two: $A^{\mu\nu} = \partial_\alpha u^\mu\, \partial^\nu u^\alpha$ is one such term), most of them will not be symmetric nor satisfy the orthogonality constraint (2.11). Not all is lost though. First, observe that any rank-one symmetric tensor $A^\mu$ can be made $u$-orthogonal simply by subtracting off its projection onto the $u$ vector:

$$\begin{aligned} A'^\mu &= A^\mu + u^\mu\, A^\alpha u_\alpha \\ &= A_\alpha\, (\eta^{\mu\alpha} + u^\mu u^\alpha) \end{aligned} \tag{2.12}$$

The "plus" sign in place of a "minus" accounts for the fact that $u^\mu u_\mu = -1$. The combination $\eta^{\mu\nu} + u^\mu u^\nu$ that projects onto $u$-orthogonal tensors occurs so frequently that we give it a name:

$$P^{\mu\nu} = \eta^{\mu\nu} + u^\mu u^\nu \tag{2.13}$$

Second, we can proceed similarly if $A^{\mu\nu}$ is a symmetric rank two tensor and project each of its components individually:

$$A'^{\mu\nu} = A_{\alpha\beta}\, P^{\alpha\mu}\, P^{\beta\nu} \tag{2.14}$$

If $A^{\mu\nu}$ is a tensor with no symmetries, we can simply symmetrize its indices after contracting with $O$. While straightforward, it is interesting to note that the symmetrization can be performed as a tensor contraction:

$$\begin{aligned} A^{(\mu\nu)} &= A^{\alpha\beta} \left( \frac{1}{2} P_\alpha{}^\mu\, P_\beta{}^\nu + \frac{1}{2} P_\alpha{}^\nu\, P_\beta{}^\mu \right) \\ &\equiv A^{\alpha\beta}\, \Pi^{\mu\nu}{}_{\alpha\beta} \end{aligned} \tag{2.15}$$

One quickly verifies that $P^{\mu\nu} u_\nu = 0$ and $P^\mu{}_\alpha\, P^{\alpha\nu} = P^{\mu\nu}$, so $P$ is indeed a linear projector. By definition, $\Pi^{\mu\nu}{}_{\alpha\beta}$ shares those properties as well.

Classification of the higher-order contributions to the stress-energy tensor is now straightforward. We simply write down every Lorentz covariant product of fluid velocity and its derivatives and ensure its $u$-orthogonality and symmetry by contracting with $\Pi^{\mu\nu}{}_{\alpha\beta}$.

## 2.2 Conformal hydrodynamics

The rest of the paper will be concerned with hydrodynamics of systems that exhibit symmetry under rescalings. More precisely, we will consider transformations of the metric of the following form:

$$g_{\mu\nu} \longrightarrow \bar{g}_{\mu\nu} = e^{2\phi(x)}\, g_{\mu\nu} \tag{2.16}$$

Such transformations are known as *Weyl* or *conformal* and are seen to modify the notion of length in the system: $g^{\mu\nu}$ measures distance in the sense that $ds^2 = g_{\mu\nu}\, dx^\mu\, dx^\nu$, and so upon rescaling (2.16) the distances grow by a factor of $e^{\phi(x)}$. The rescaling (2.16) is not a coordinate transformation, but instead a "forceful" stretching of the physical system by a space-dependent factor. The peculiar form of the factor $e^{2\phi(x)}$ is chosen in such a way that when $\phi(x)$ is a smooth function, the factor is smooth and positive. In particular, the factor is never zero, so the transformation never introduces any "pathologies". Furthermore, it maps light cones to themselves, lightlike vectors to lightlike vectors, and spacelike vectors to spacelike vectors, so that the causal structure of the manifold is preserved.

In general, $\phi(x)$ is allowed to vary as a function of the manifold coordinates, but even then locally the transformation never mixes components of $g$ nor scales them by unequal amounts. In particular, if $e_1$ and $e_2$ are coordinate vectors normalized to unity so that $e_i \to e^{-\phi(x)}\, e_i$, their scalar product is preserved:

$$e_1^\mu\, e_2^\nu\, g_{\mu\nu} \longrightarrow \bar{e}_1^\mu\, \bar{e}_2^\nu\, \bar{g}_{\mu\nu} = e_1^\mu\, e_2^\nu\, g_{\mu\nu} \tag{2.17}$$

We conclude that conformal transformation preserve angles. In the special case when $\phi =$ const the transformation is a simple and easy to visualize rescaling by a constant factor. For this reason we will often refer to general conformal transformations simply as "rescalings".

As the metric tensor is used to measure norms of tensors, a Weyl transformation must be followed by an appropriate rescaling of tensor quantities, lest the physical content of the theory change more than just by the distance scale. In our case of interest, we must ensure that the relativistic velocity is properly normalized: $u^\mu\, u_\mu = -1$. We therefore find that we have to rescale $u$ as follows:

$$u^\mu \longrightarrow \bar{u}^\mu = e^{-\phi(x)}\, u^\mu \tag{2.18}$$

Derivatives in the rescaled theory can be related to derivatives prior to applying of the transformation. Since in general $\phi = \phi(x)$ so that the metric becomes space dependent we can work out this relation by requiring that the derivatives are covariant with respect to the metric. The result is [5]:

$$\begin{aligned} \bar{\nabla}_\mu x^\nu &= \nabla_\mu x^\nu + A^\nu{}_{\mu\alpha}\, x^\alpha \\ \bar{\nabla}_\mu \omega_\nu &= \nabla_\mu \omega_\nu - A^\alpha{}_{\mu\nu}\, \omega_\alpha \end{aligned} \tag{2.19}$$

where

$$A^{\alpha}{}_{\mu\nu} = 2\,\delta^{\alpha}{}_{(\mu}\partial_{\nu)}\phi(x) - g_{\mu\nu}\,g^{\alpha\beta}\,\partial_{\beta}\phi(x) \tag{2.20}$$

plays a role of a connection, in that it measures the difference between the two derivatives.

Any tensor that rescales with an overall constant $e^{w\phi(x)}$ is said to transform *homogeneously* with a weight $w$. It is easy to see that while, for example, $P^{\mu\nu} = g^{\mu}\nu + u^{\mu}u^{\nu}$ has just the right structure to transform homogeneously, there are tensors, such as $\delta^{\nu\mu} + u^{\nu}u^{\mu}$ that do not. A theory with a dynamical equation that transforms homogeneously under a conformal transformation of the metric and appropriate transformations of the dynamical variables is said to be *conformally invariant*, or simply *conformal*. Physically, conformal invariance is a property of theories whose dynamics *look alike* at different length scales, provided that we also rescale dynamical variables with appropriate weights. This is a very appealing property: if, say, galactic matter exhibited conformal symmetry, one could predict galactic dynamics on the scale of billions of years by conducting a small scale experiment with a conformal fluid of similar stress-energy structure, but at appropriately scaled thermodynamic conditions.

In accordance to the above discussion, a conformal hydrodynamic theory must satisfy two conditions: under a conformal transformation (2.16) the stress-energy tensor must transform homogeneously, and the equations of motion must remain invariant. Given $\partial_{\mu}T^{\mu\nu} = 0$ we must have:

$$T^{\mu\nu} \longrightarrow \bar{T}^{\mu\nu} = e^{w\phi(x)}\,T^{\mu\nu} \tag{2.21}$$

as well as

$$\begin{aligned} 0 = \bar{\partial}_{\mu}\bar{T}^{\mu\nu} &= \partial_{\mu}\left(e^{w\phi(x)}\,T^{\mu\nu}\right) + A^{\mu}{}_{\mu\alpha}\,e^{w\phi(x)}\,T^{\alpha\nu} + A^{\nu}{}_{\mu\alpha}e^{w\phi(x)}\,T^{\mu\alpha} \\ &= e^{w\phi}\left(\,\partial_{\mu}T^{\mu\nu} + (w+d+2)\,\partial_{\mu}\phi(x)\,T^{\mu\nu} - \partial^{\nu}T^{\mu}{}_{\mu}\,\right) \end{aligned} \tag{2.22}$$

In the latter constraint, the first term vanishes by the assumed conservation equation, whereas the remaining two terms impose the following constraints:

$$\begin{aligned} w &= -(d+2) \\ T^{\mu}{}_{\mu} &= 0 \end{aligned} \tag{2.23}$$

It is interesting to note that imposing of the conformal symmetry ties the conformal weight of $T^{\mu\nu}$ to the spacetime dimensionality $d$.

### 2.2.1 Conformal ideal fluid

The requirements (2.23) imposed by conformal symmetry can be readily implemented in the ideal fluid of Sec. 2.1.1. The tracelessness of the stress energy tensor supplies a ther-

modynamic equation of state:

$$T^{\mu}{}_{\mu} = 0 \implies \rho = p\,(d-1) \tag{2.24}$$

It will be convenient in the remaining part of the paper to express the energy density $\rho$ as a function of thermodynamic temperature. There are two ways to do this. We could either perform a dimensional analysis and compare energy dimensions: $[\,T^{\mu\nu}\,] = d$, $[\,u^{\mu}\,] = 0$ so that $[\,\rho\,] = d$. Since $[\,T\,] = 1$ and there are no other dimensionful parameters in the theory, we must have that:

$$\rho \propto T^{d} \tag{2.25}$$

A more physical way of arriving at this result is to consider conformal scaling of terms occurring in the Gibbs-Duham equation. See [16] for a detailed discussion.

After the smoke clears, the ideal conformally symmetric stress energy tensor becomes:

$$T_0^{\mu\nu} = \alpha\, T^{d}\,(\eta^{\mu\nu} + d\, u^{\mu}\, u^{\nu}) \tag{2.26}$$

In order to satisfy homogeneity of $T^{\mu\nu}$ under conformal transformations in eq. (2.21), we need to impose scaling of $T$. Investigating eq. (2.26) above, we see that the conformal weight of $T$, $w(T)$ is $w(T) = (\,w(T^{\mu\nu}) - 2w(u)\,)^{-d} = -1$.

In summary, we have created a tensorial description of $0^{\text{th}}$ order fluid dynamics with fundamental variables $u$ and $T$ and dynamical equations that remain invariant under rescalings of the metric, provided we impose conformal weights of the fluid variables as follows:

$$\begin{aligned} u^{\mu} &\longrightarrow e^{-\phi(x)}\, u^{\mu} \\ T &\longrightarrow e^{-\phi(x)}\, T \end{aligned} \tag{2.27}$$

### 2.2.2 Conformal fluid at higher orders

We are now in the position to consider all possible contributions to the stress energy tensor compatible with conformal symmetry. In the previous section, we learned that a conformal stress energy tensor is traceless. Since terms with different number of derivatives are separated by an order of magnitude, it must be true that each individual term in $T^{\mu\nu}$ is traceless. We modify the $\Pi$ projector constructed in Sec. 2.1.2 so that in addition to symmetrization and projection, it also subtracts the trace:

$$\Pi^{\mu\nu}{}_{\alpha\beta} = \left(\frac{1}{2}P_{\alpha}{}^{\mu}\, P_{\beta}{}^{\nu} + \frac{1}{2}P_{\alpha}{}^{\nu}\, P_{\beta}{}^{\mu} - \frac{1}{2}P^{\mu\nu}\, P_{\alpha\beta}\right) \tag{2.28}$$

One easily verifies that $\Pi^{\mu}{}_{\nu\alpha\beta}$ and that the new piece is $u$-orthogonal.

# Chapter 3

# Geometry of the AdS space

Anti de Sitter spaces (AdS) arise as vacuum solutions to Einstein field equations with a negative cosmological constant. AdS spaces have attracted popularity in theoretical physics due to the cherished conjecture that relates conformal field theories to string theories on AdS background [7]. In particular, in this paper we explore a realization of the conjecture whereby a classical conformal fluid is shown to encode dynamics of a black hole on AdS background. It will be useful to briefly review basic geometrical properties of AdS and asymptotically AdS spaces to develop an intuitive feeling before delving into calculations.

## 3.1 AdS Defined

Anti de Sitter space is a maximally symmetric homogeneous space with constant negative curvature. In this regard, Minkowski space can be regard pictorially as a limit of AdS spaces as the constant curvature approaches 0.[1]

To gain insight into the negative curvature of the Anti de Sitter space, we will consider the AdS space as the embedding of a quadratic surface in flat space with signature $(-,-,+,+,+,\dots)$. For concreteness and ease of visualization, we will work with $1+1$ dimensional AdS, but most of the construction generalizes to arbitrary dimension unless noted.

We will construct the AdS space as a hyperboloid in a 3-dimensional flat manifold with metric:

$$ds^2 = -\mathrm{d}u^2 - \mathrm{d}v^2 + \mathrm{d}a^2 \tag{3.1}$$

The 2-dimensional hyperboloid is defined as the locus of the following equation:

$$-u^2 - v^2 + a^2 + R_{\mathrm{AdS}}^2 = 0 \tag{3.2}$$

The locus describes a hyperboloid of one sheet with the revolution axis along the $u = v = 0$

[1]This statement should be treated informally, as the "limit" is non-trivial: the isometry group of AdS $SO(2, n-1)$ undergoes a contraction to the Poincaré group of Minkowski space.

line. To see that this construction induces the correct Lorentzian $(-,+,+)$ metric, we solve the hyperboloid equation by introducing coordinates $(t,\rho)$ through the following implicit relations [6]:[2]

$$\begin{aligned} u &= R_{\text{AdS}}\,\sin(t)\,\cosh(\rho) \\ v &= R_{\text{AdS}}\,\cos(t)\,\cosh(\rho) \\ a &= R_{\text{AdS}}\,\sinh(\rho) \end{aligned} \tag{3.3}$$

For the $1+1$ dimensional case, the induced metric becomes:

$$ds^2_{\text{AdS}_{1+1}} = R^2_{\text{AdS}}\left(-\cosh^2\rho\,\mathrm{d}t^2 + \mathrm{d}\rho^2\right) \tag{3.4}$$

With this choice, we have traded the $a$ space-like coordinates for spherical coordinates with the radial direction $r^2 = \sinh^2(\rho)$. The remaining two time-like coordinates are reduced to a single *circular* time-like coordinate via the constraint. As can be easily checked, slices of the hyperboloid with a plane constitute geodesics of the AdS space. *Timelike* geodesics, in turn, are sections for which $\mathrm{d}t > \mathrm{d}x$, which are seen to form ellipses. Our construction contains closed time-like loops! The fact that every timelike geodesic is closed motivates describing the AdS space as *attractive*: every physically realizable trajectory comes back to itself, as if under the action of an attractive potential. In fact, the $1+1$ AdS space is special in that the closed time-like geodesics can be removed by taking the universal cover, which is impossible for the general $n+1$ with $n>1$ dimensional case [10]. We conclude that for $n>1$ the AdS space has the topology of $\mathbf{S}^1\times\mathbb{R}^n$.

When imagining the AdS space as a hyperboloid, one needs to remember that the signature of the embedding space is $(-,-,+)$ and not Euclidean, as one might naively conclude having drawn a hyperboloid on a piece of paper. While the naive Euclidean picture suggests that curvature is variable and greatest at $\rho=1$, this is not the case: one need to take the signature into consideration.

The AdS space has a timelike conformal boundary [10]. To wit, compare the asymptotic behavior of AdS in our hyperboloid coordinates to regular Minkowski space. In flat space, for every unit proper time, a light ray covers an equivalent spacelike distance; the conformal infinity is a point. In AdS, however, the same light ray covers $\rho\,\mathrm{d}r^2$, which grows without bound at $\rho\pm\infty$; the conformal boundary is a timelike surface. For this reason, AdS is does not admit Cauchy surfaces: information can "flow in" and "out" at the boundary. A different coordinate system which makes the conformal boundary manifest is one which puts the radial dimension on a compact domain, $\cosh(\rho)=\frac{1}{\cos r}$, with $r\in(0,\pi/2)$, so that the metric becomes:

$$ds^2 = \frac{R^2_{\text{AdS}}}{\cos^2 r}\left(-\mathrm{d}t^2+\mathrm{d}r^2\right) \tag{3.5}$$

[2] One could extend this construction to higher dimension by noticing that the hyperboloid is spherically symmetric in the spacetime dimensions and introducing the standard spherical coordinates.

The boundary is now approached as $r \to \pi/2$.

Finally, we bring the AdS metric into the form we will use throughout the rest of the paper. In doing so, the transverse coordinates receive different treatment from the radial coordinate $\rho$, so we will move our discussion up a dimension. The hyperboloid is now a 3-dimensional surface defined by the equation:

$$-u^2 - v^2 + a^2 + b^2 + R_{\text{AdS}}^2 = 0 \tag{3.6}$$

The Poincaré coordinates are obtained via:

$$\begin{aligned} u &= \frac{r}{2\,R_{\text{AdS}}}\left(R_{\text{AdS}}^2 + s\right) \\ v &= t \\ a &= x \\ b &= \frac{r}{2\,R_{\text{AdS}}}\left(R_{\text{AdS}}^2 - s\right) \end{aligned} \tag{3.7}$$

with

$$s = -t^2 + x^2 \tag{3.8}$$

The resulting metric is:

$$ds^2 = \frac{R_{\text{AdS}}^2}{z^2}\left(-\mathrm{d}t^2 + \mathrm{d}x^2 + \mathrm{d}y^2 + \mathrm{d}z^2\right) \tag{3.9}$$

## 3.2 Anti de Sitter black hole

Schwartzchild-like black hole solutions to Einstein field equations with negative cosmological constant can be found in a manner analogous to flat space [5], [9]. The results in $d+1$ dimensions are remarkably similar to the flat space black hole when expressed in Poincaré coordinates:

$$ds^2 = -r^2\, f\,(br)\ \mathrm{d}t^2 + \frac{\mathrm{d}r^2}{r^2\, f(br)} + r^2\,\mathrm{d}\mathbf{x}^2 \tag{3.10}$$

where

$$f(r) = 1 - \frac{1}{r^d} \tag{3.11}$$

and $b = 1/R_{\text{BH}}$ is a constant controlling the radius of the black hole horizon.

Throughout the remainder of this paper we will be working with AdS black holes expressed in *null* Eddington-Finkelstein coordinates that are explicitly regular at the horizon. The Poincaré coordinates (3.10) can be brought into the null form by the following coordinate transformation. First, we notice that null paths satisfy $ds^2 = 0$:

$$\frac{dt}{dr} = \frac{1}{r^2}\, f(br)^{-1} \tag{3.12}$$

Had the $dt/dr$ factor been simply 1, a redefinition $\nu = t + r$ would suffice. In the present case, we put $\nu = t + \mathcal{F}(r)$ and require that the $\mathrm{d}r^2$ component of the resulting metric vanishes. Demanding in addition that $\mathrm{d}\nu\,\mathrm{d}r > 0$ (in-falling null coordinates) constitutes a differential equation for $\mathcal{F}(r)$, which can be solved to find::

$$\begin{aligned} \nu &= t + b\,\mathcal{F}(r) \\ \mathcal{F}(r) &= -\tfrac{\sqrt{3}}{3}\,\tan^{-1}\left(\tfrac{\sqrt{3}}{3}\,(2r+1)\right) + \tfrac{1}{6}\log\left(\tfrac{(1-r)^2}{1+r+r^2}\right) \end{aligned} \tag{3.13}$$

The resulting metric takes the following form:

$$ds^2 = 2\,\mathrm{d}t\,\mathrm{d}r - r^2 f(br)\,\mathrm{d}t^2 + r^2\,\mathrm{d}\mathbf{x}^2 \tag{3.14}$$

## 3.3 Brown-York stress-energy tensor

Energy and momentum of the gravitational field in general relativity are a hairy subject. With the diffeomorphism invariance built in into the very foundation of the theory, it is impossible to give a sensible covariant definition of a local energy-momentum density when the only "covariant" information different observers agree on is that what they are looking at is vacuum. The Brown-York tensor is a non-local answer to the question of gravitational energy: computed at the boundary (infinity) of the spacetime, it quantifies the impact of deformations of space on regions of space that are infinitely far away. To see that the boundary should play an important role in the considerations of gravitational energy, consider how one would set up a variation-of-action procedure to obtain Einstein's equations of motion. An action that correctly reproduces the field equations upon varying with respect to $g_{\mu\nu}$ is the cherished Einstein-Hilbert action:

$$S_{GR} = -\frac{1}{16\,\pi\,G}\int d^{d+1}x\,\sqrt{-\det g}\,(R - \Lambda) \tag{3.15}$$

A blind application of the Euler-Lagrange equations recovers Einsteins equations but misses an important point: that the variation of the action does not necessarily vanish at the "boundaries" of the integral, as necessary for the commonplace ignoring of boundary terms arising in deriving of the Euler-Lagrange equations. It should not be surprising that the boundary terms cannot be neglected even for non-compact spaces. Even if one uses compact coordinates, the action integral is performed with respect to the manifold volume measure and hence coordinate-invariant. The boundary contribution can be shown to take the following form:

$$S_{\partial M} = -\frac{1}{8\,\pi\,G}\int_{\partial_M} d^d x\,\sqrt{-\det\gamma}\,\Theta \tag{3.16}$$

where $\gamma$ is the boundary metric and $\Theta$ is its extrinsic curvature, defined as:

$$\Theta^{\mu\nu} = -\frac{1}{2}\left(\nabla^{\mu}\hat{n}^{\nu} + \nabla^{\nu}\hat{n}^{\mu}\right) \tag{3.17}$$

with $\hat{n}$ being the unit normal vector to $\gamma$. All of the quantities participating in the above expressions need to be defined and/or computed through a limiting procedure. Recalling that the classical action measures $T - V$, the non-vanishing of the boundary term suggests that the boundary metric captures some of the aspects of gravitational field's potential energy.

The Brown-York stress energy tensor is defined as the variation of the action with respect to the boundary metric:

$$T^{\mu\nu} = \frac{\delta}{\delta\gamma_{\mu\nu}} S_{\partial M} \tag{3.18}$$

The above construction is analogous to how would arrive at a stress energy tensor for an ordinary matter field coupled to gravity [5], for if one adds a matter term such as $S_{\text{matter}} = \int dx^{d+1}\sqrt{g}\,\mathcal{L}[\phi]$ term to eq. (3.15), taking functional derivatives with respect to $g_{\mu\nu}$ would produce a rank two tensor contribution to the Einstein field equations that we would interpret as $T^{\mu\nu}$ of $\phi$. The stress-energy tensor computed in accordance to the above prescription for an AdS black hole is divergent. The divergences have been understood to arise as manifestations of ultraviolet divergences of the field theory dual in the AdS/CFT sense, and can be removed by a procedure that is believed to be dual to the field theory renormalization. The prescription of [17] calls for an addition of counter-terms to the bulk geometry action. Requiring that the divergent pieces of the Brown-York tensor are canceled specifies the countertenor's uniquely (see [17] for details). The terms are found to vary depending on the dimensionality of space, and in our present case of interest of $3+1$ AdS are:

$$S_{\text{ct}} = -\int_{\partial M} \frac{2}{l}\sqrt{-\det\gamma}\left(1 - \frac{l^2}{4}R\right) \tag{3.19}$$

where $l$ is a length characterizing the curvature of vacuum AdS space related to the cosmological constant $\Lambda$ as:

$$\Lambda = -\frac{d}{d-1}2l^2 \tag{3.20}$$

Having added the counter terms corrections, the re-normalized Brown-York stress-energy tensor becomes:

$$T^{\mu\nu}_{\text{BY}} = \frac{1}{8\pi G}\left(\Theta^{\mu\nu} - \Theta\,\gamma^{\mu\nu} - 2\,\gamma^{\mu\nu} - G^{\mu\nu}\right) \tag{3.21}$$

# Chapter 4

# Fluid-gravity correspondence

In this section we construct an explicit realization of the holographic principle between classical gravity and a conformal fluid. The main result will be a description of an out of the equilibrium $3+1$ dimensional black hole on an AdS background written covariantly in terms of a set of functions $T$ and $u^\mu$ that we will interpret as temperature and velocities of a $2+1$ dimensional conformal fluid. Einstein field equations of the gravitational system will be shown to be equivalent to conservation equations of the fluid stress energy tensor. Moreover, the gravity description will be organized in a derivative expansion in a manner reminiscent of the hydrodynamical expansion of the stress-energy tensor (2.6):

$$g_{\mu\nu} = g^{(0)}_{\mu\nu}(T,u) + g^{(1)}_{\mu\nu}(T,u,\partial u) + g^{(2)}_{\mu\nu}(T,u,\partial u,\partial^2 u) + \cdots \tag{4.1}$$

Higher order terms will be calculated from a perturbation expansion in the order of derivatives of $u$.

We specialize our derivation to the case of $3+1$ dimensional gravity and—equivalently—a $2+1$ dimensional fluid for pragmatic reasons. First, analytical computations involving 4-dimensional metric and 3-dimensional fluid tensors, while done on a computer, will still be tractable by eye. Second, we will ultimately simulate numerically the lower-dimensional hydrodynamic theory and construct the black hole geometry numerically. The time and space requirements of such endeavor grow exponentially in the number of spacetime dimensions, and a simple counting shows that $3+1$ dimensions are adequately manageable on a personal-grade computer. [1]

The analysis of this section follows previous works [13], [14], and [19] closely. Refs. [13] and [19] carry a detailed analysis for $4+1$ dimensional gravity, while [14] reduces the analysis to $3+1$ dimensions.

[1] Assuming about $N = 50$ collocation points in all spacelike dimensions for sufficient numerical accuracy, memory required to store $\frac{d(d+1)}{2} \approx d^2$ components of the various GR tensors of interest at each time step is about $N^{d-1} \times d^2 \times 8$ bytes, which is roughly 7 MB for $d = 3+1$, and 0.6 GB for $d = 4+1$. Given that computation of the GR tensors requires knowledge of time derivatives of the metric, one needs to hold in memory not one but several time steps at a time.

The results of our calculation agree almost exactly with [14], except for a difference in the scalar $SO(2)$ sector of the metric.

## 4.1 Black hole in equilibrium

Our starting point is a vacuum solution to Einstein equations with constant negative curvature, introduced in Sec. 3 in eq. (3.14), specialized to $3+1$ dimensions:

$$ds^2 = 2\,\mathrm{d}t\,\mathrm{d}r - r^2 f(br)\,\mathrm{d}t^2 + r^2\,\mathrm{d}\mathbf{x}^2 \tag{4.2}$$

where in $3+1$ dimensions $\mathrm{d}\mathbf{x}^2$ stands for two spacetime directions, and $f(r)$ and $b$ stand for:

$$\begin{aligned} f(r) &= 1 - \frac{1}{r^3} \\ b &= \frac{3}{4\pi T} \end{aligned} \tag{4.3}$$

with $T$ being the black hole temperature. One readily verifies that this is a solution of Einstein equations with cosmological constant $\lambda = 3$:

$$R_{MN} - \tfrac{1}{2} g_{MN} R + \lambda g_{MN} = 0 \tag{4.4}$$

Taking the trace we discover $R = -12$. As explained in section 3, the apparent horizon is a spacelike surface with $r = 1/b$.

The first step is to parametrize the metric in eq. (4.2) by a set of parameters $u^\mu$ that we will eventually identify with the fluid relativistic velocity. Such $u^\mu$ must be Lorentz-covariant when viewed as a vector in a $2+1$ dimensional flat Minkowski space, and its covariance must be respected by the metric. Indeed, we observe that the black hole metric in eq. (4.2) is a modification of pure $\mathrm{AdS}_5$, and that the metric retains the $SO(1,2)$ subgroup of the full $\mathrm{AdS}_5$ isometry group $SO(2,3)$. This is manifested in our choice of coordinates: constant $r$ slices look like Minkowski spaces. The observation provides a hint for parametrizing the metric in terms of the fluid velocity $u^\mu$: perform a $SO(1,2)$ coordinate transformation parametrized by the constant 3-velocity $u$, or in other words, boost the metric by $u$:

$$\begin{aligned} \mathrm{d}t &\longrightarrow \gamma\,(\mathrm{d}t - \mathrm{d}\mathbf{x}\cdot\mathbf{v}) = -u_\mu\,\mathrm{d}x^\mu \\ \mathrm{d}x^i &\longrightarrow \mathrm{d}x^i + v^i\left(\frac{\gamma-1}{v^2}\mathrm{d}\mathbf{x}\cdot\mathbf{v} - \gamma\,\mathrm{d}t\right) = \mathrm{d}x^i + \frac{u^i}{u^t+1}\mathrm{d}\mathbf{x}\cdot\mathbf{u} - u^i\,\mathrm{d}t \end{aligned} \tag{4.5}$$

so that after some algebra:

$$\mathrm{d}\mathbf{x}^2 = (\eta_{\mu\nu} + u_\mu u_\nu)\,\mathrm{d}x^\mu\,\mathrm{d}x^\nu = P_{\mu\nu}\,\mathrm{d}x^\mu\,\mathrm{d}x^\nu \tag{4.6}$$

The resulting boosted metric becomes:

$$ds^2 = -2\,u_\mu\,\mathrm{d}x^\mu\,\mathrm{d}r - r^2 f(r)\,u_\mu u_\nu\,\mathrm{d}x^\mu\,\mathrm{d}x^\nu \;\; + r^2\,P_{\mu\nu}\,\mathrm{d}x^\mu\,\mathrm{d}x^\nu \tag{4.7}$$

Caution should be taken to the meaning of indices in the expression above. Greek indices have been introduced to keep track of the components of the 3-velocity and their contractions with 3-indices of four dimensional vectors in a shorthand fashion that is also consistent with Lorentz contraction in a $2+1$ dimensional Minkowski space. The Greek indices are not manifold indices and should not be raised with the manifold metric: it is not true that $u_\mu = g_{\mu\nu}\,u^\nu$ but rather $u_\mu = \eta_{\mu\nu}\,u^\nu$. Attention needs to be paid when one rewrites any expressions that appear in this chapter and changes position of the Greek indices – one needs to resist the urge to raise and lower them with the full manifold metric. Alternatively, one can read of components of $g_{\mu\nu}$ from eq. (4.7) and consider position of the Greek indices set in stone and never worry about it.

## 4.2 Out-of-equilibrium black hole

The boosted black hole is clearly a solution to the Einstein field equations. It also has the desired feature of depending parametrically on constant $u^\mu$, as well as the black hole temperature $T$. We now promote $u^\mu$ and $T$ to functions of the transverse coordinates (also referred to as boundary coordinates in some literature), and impose the hydrodynamic assumption of size hierarchy of space-time derivatives of $u$ and $T$. In general, the resulting metric is not a valid gravity solution, for we have introduced arbitrary coordinate dependence into its functional form. We can nevertheless *correct* the form of eq. (4.7) as well as impose additional constraints on $u^\mu$ in hope of making the resulting geometry a *better* solution, in a sense that we will soon make precise. To this end, we observe that corrections to the form of eq. (4.7) must depend on gradients of $u$: as we take $u$ to vary on longer and longer length scales, the metric corrections must vanish so that in the limit of constant $u$ we are back to eq. (4.7). We therefore postulate that it is possible that corrections to the metric be enumerated by the number of derivatives of $u$, and that they diminish in importance as the number of derivatives grows:

$$g_{\mu\nu} = g^{(0)}_{\mu\nu}(T,u) + g^{(1)}_{\mu\nu}(T,u,\partial u) + g^{(2)}_{\mu\nu}(T,u,\partial u,\partial^2 u) + \cdots \tag{4.8}$$

Now, as each term of the above "expansion" differs in magnitude, we can truncate the series at a desired order $n$, evaluate on it the Einstein equations, and demand that the truncated metric satisfies the equations up to errors of order $n+1$ in the number of derivatives. We can then repeat this calculation order by order and obtain more and more accurate approximations of the true solution.

In particular, we observe that order 0 metric solves Einstein equations up to order 1

trivially – all of the error terms produced by derivatives in Einstein equations are necessarily order 1 and higher. We now outline an iterative procedure that allows us to improve the solution. Assuming that we have already constructed a solution to Einstein equations $G^{N-1}$ valid up to errors of order $\mathcal{O}(\partial^n u)$, we can now add the $n^{\text{th}}$ order term $g^{(n)}_{\mu\nu}$ and relax the error order to $\mathcal{O}(\partial^{n+1}u)$. Einstein field equations evaluated on $G^n = G^{n-1} + g^{(n)}_{\mu\nu}$ give rise to three kinds of terms: those that vanish by the design of $G^{n-1}$, and an additional contribution at order $\mathcal{O}(\partial^{n+1}u)$. Of the latter, we expect to find a piece coming from taking $r$ derivatives of the new and undetermined order $n$ term, possibly contracted with terms of order no higher than 0. These equations constrain the $r$ dependence of the undetermined order $n$ contribution to the metric and decide on its tensor structure (how derivatives of $u$ fit together). For this reason, we will call those the "constraint equations". We also expect a piece coming from taking both spatial and $r$ derivatives $\partial_\mu$ of the lower order contributions to $g_{\mu\nu}$ that have already been solved for. This piece which does not include the undetermined $g^{(n)}$. These equations are at heart of the fluid-gravity correspondence: we will find that the $g^{(n)}$-independent equations constitute precisely the conservation equations of the $2+1$ dimensional conformal Brown-York boundary stress energy tensor *constructed out of* the order $n-1$ solution obtained at previous order:

$$\partial_\mu \left(T^{\mu\nu}_{\text{BY}}\right)^{(n-1)} = 0 \tag{4.9}$$

Those equations specify the dynamics of the fluid, and equivalently, of the black hole, for which reason we will refer to them as "dynamical equation". We will come back to the computation of the Brown-York tensor and the verification of the fluid equations at the end of the computation, when we will have obtained the metric solution.

Summarizing the discussion of the metric constraint equations, we expect that the field equations evaluated on $G^N$ will give rise to a differential equation of the following form [19]:

$$\mathbb{H}\Big[\, g^{(0)}(T,u)\,\Big] g^{(n)} = S^{(n)} \tag{4.10}$$

where $\mathbb{H}$ is a local differential operator in $r$ which depends on the zeroth order metric alone, $g^{(n)}$ is the undetermined contribution to the metric at order $n$, and $S^{(n)}$ are $n^{\text{th}}$ order terms which do not include $g^{(n)}$. Moreover, as Einstein field equations are second order, we expect $\mathbb{H}$ to be at most second order in $r$ derivatives.

The AdS black hole Eddington-Finkelstein coordinates used in this analysis shed some light on the physical meaning of the perturbative calculation outlined above. Suppose that there are regions of the transverse coordinates where gradients of $u$ are small or practically negligible, which we also interpret as regions where the dual fluid is locally equilibriated. Then in that local neighborhood, the solution reduces to the black hole metric (4.7) *everywhere* in a tube-like region along the $r$ coordinate. Therefore, the perturbative corrections constitute curvature of spacetime required to seam those locally equilibriated regions into

a manifold in a manner consistent with Einstein gravity.

To proceed further, we need a reasonable guess for the functional form of $g^{(i)}_{\mu\nu}$. It will be most useful to fix a convenient gauge consistent with our $0^{\text{th}}$ order solution. Let us investigate the available gauge freedom. We observe that we can always remove the $rr$ component by a simultaneous redefinition of $r$ and $t$, locally rescale the $r\mu$ coordinates by redefinition of $x^\mu$ subject to $ds^2 = 0$, and we are still left with one degree of freedom [13]. Therefore, using the gauge freedom we can impose the following constraints:

$$\begin{aligned} g_{rr} &= 0 \\ g_{\mu r} &\propto u_\mu \\ g^{(0),MN} g^{(n)}_{MN} &= 0 \end{aligned} \tag{4.11}$$

In addition, as $g^{(0)}_{\mu\nu}$ is a symmetric 2-tensor under $SO(2)$, we can always choose coordinates which make the scalar, vector, and symmetric traceless tensor representations (**5**) of $SO(2)$ manifest. The only possible expression that satisfies the gauge and symmetry requirements is:

$$\begin{aligned} (ds^2)^{(n)} = \frac{k^{(n)}}{r^2} u_\mu u_\nu \, \mathrm{d}x^\mu \, \mathrm{d}x^\nu - 2\, h^{(n)} u_\mu \, \mathrm{d}x^\mu \, \mathrm{d}r - r^2 \, h^{(n)} P_{\mu\nu} \, \mathrm{d}x^\mu \, \mathrm{d}x^\nu \\ -\frac{1}{r}\left(j^{(n)}_\nu u_\mu + j^{(n)}_\mu u_\nu\right) \mathrm{d}x^\mu \, \mathrm{d}x^\nu + r^2 \, \alpha^{(n)}_{\mu\nu} \, \mathrm{d}x^\mu \, \mathrm{d}x^\nu \end{aligned} \tag{4.12}$$

All of the undetermined functions $h^{(n)}$, $k^{(n)}$, $j^{(n)}_\mu$, $\alpha^{(n)}_{\mu\nu}$ are functions of $n$ derivatives of $u^\mu$ and $b$ and depend on the transverse spacetime coordinates only through $u^\mu$ and $b$. Using remaining gauge freedom we demand that:

$$\begin{aligned} u^\mu \, j_\mu &= 0 \\ u^\mu \, \alpha_{\mu\nu} &= 0 \end{aligned} \tag{4.13}$$

If one computes the contribution of the $n^{\text{th}}$ order piece (4.12) to the Brown-York stress-energy tensor (3.21), the above choices guarantee that the contribution is $u$-orthogonal:

$$u^\mu \, T^{\mu\nu}_{\text{BY}} = 0 \tag{4.14}$$

As discussed in Sec. 2, orthogonality of the higher-order contributions to the stress-energy tensor is required by the definition of $u$ as the four velocity of the fluid in the observer's frame of reference. Coordinate diffeomorphisms involving $j$ and $\alpha$ that change (4.13) correspond to re-definitions of $u$.

## 4.3 Analytical calculation

Performing the perturbative calculation covariantly is a task of daunting complexity. Nevertheless, we can take advantage of the locality of the expected differential equations and solve the equations point by point in a convenient frame of reference. The simplest choice is naturally to solve the equations in the neighborhood of $x^\mu = 0$ in a local (or stationary) fluid frame where $u^\mu = (1, 0, 0)$, $b = 1$ and derivatives of $u$ are given in terms of observer's velocities:

$$\begin{aligned} u^t(x^\mu) &= \frac{1}{\sqrt{1 - v_x(x^\mu)^2 - v_y(x^\mu)^2}} \\ u^i(x^\mu) &= \frac{v^i}{\sqrt{1 - v_x(x^\mu)^2 - v_y(x^\mu)^2}} \end{aligned} \tag{4.15}$$

The choice is equivalent to a choice of a particular coordinate system, so we should not expect the results to come out Lorentz-covariant. Nevertheless, given an expression in the local coordinate system we can always "covariantize", or find the general tensor expression whose local form is the given expression.

As discussed before, the $0^{\text{th}}$ order metric is a solution of Einstein equations to $1^{\text{st}}$ order in derivatives. To facilitate calculations of the $n^{\text{th}}$ order $g^{(n)}_{\mu\nu}$ in the local frame, we Taylor-expand the solution from previous orders in $x^\mu$, keeping terms up to the desired order $n$, and setting $u^\mu = (1, 0, 0)$ at the end. In particular, at first order the input to the Einstein field equations in the local frame becomes:

$$\begin{aligned} ds^2 = {} & 2\,\mathrm{d}t\,\mathrm{d}r - r^2 f(br)\,\mathrm{d}t^2 + r^2\,\mathrm{d}\mathbf{x}^2 \\ & -\frac{3}{r^2}\,x^\mu\,\partial_\mu b^{(0)}\,\mathrm{d}t^2 - \frac{1}{r}x^\mu\,\partial_\mu \mathbf{v}^{(0)}\cdot\mathrm{d}\mathbf{x}\,\mathrm{d}t - 2\,x^\mu\partial_\mu \mathbf{v}^{(0)}\cdot\mathrm{d}\mathbf{x}\,\mathrm{d}r \\ & \frac{k^{(n)}}{r^2}\,\mathrm{d}t^2 - 2\,h^{(n)}\,\mathrm{d}t\,\mathrm{d}r - r^2\,h^{(n)}\,\mathrm{d}\mathbf{x}^2 - \frac{2}{r}\,\mathbf{j}^{(n)}\cdot\mathrm{d}\mathbf{x}\,\mathrm{d}t + r^2\,(\alpha^{(n)})_{ij}\,\mathrm{d}x^i\,\mathrm{d}x^j \end{aligned} \tag{4.16}$$

where boldfaces stand for the spatial components of the transverse coordinates, and all functions of $v$ and $b$ are evaluated at $x^\mu = 0$. The first line in the above equation is naturally the zeroth order metric evaluated at $x^\mu = 0$ (stationary black hole), the second line contains $1^{\text{st}}$ order terms from Taylor expansions, and the third line is our ansatz for the $1^{\text{st}}$ order solution, whose $0^{\text{th}}$ order expansion in $x^\mu$ coincides with $1^{\text{st}}$ order in derivatives of $v$.

The differential operator $\mathbb{H}$ does not depend on the specific order $n$ and can in principle be read off at any order in the calculation. We have verified that $\mathbb{H}$ indeed agrees for both $1^{\text{st}}$ and $2^{\text{nd}}$ orders.

The undetermined functions $h$ and $k$, $j$, and $\alpha$ appear in different sectors of the $SO(2)$ group, and we expect that—protected by the symmetry—their respective differential equations decouple from one another. Indeed, we find that at any order the differential equations

are:

$$\begin{aligned}
\frac{1}{r^4}\frac{d}{dr}\left[r^4\frac{d}{dr}h^{(n)}(r)\right] &= S_h^{(n)}(r) \\
\frac{d}{dr}\left[-\frac{2}{r}k^{(n)}(r)+\left(1-4r^3\right)h^{(n)}(r)\right] &= S_k^{(n)}(r) \\
\frac{r}{2}\frac{d}{dr}\left[\frac{1}{r^2}\frac{d}{dr}j_i^{(n)}(r)\right] &= S_j^{(n)}(r)_i \\
\frac{d}{dr}\left[-\frac{1}{2}r^4 f(r)\frac{d}{dr}\alpha_{ij}^{(n)}(r)\right] &= S_\alpha^{(n)}(r)_{ij}
\end{aligned} \tag{4.17}$$

While the $r$ dependence has been shown explicitly, one should remember that all $h$, $k$, $j$ and $\alpha$, as well as their respective sources are functions of $n^{\text{th}}$ derivatives of the fluid velocities.

### 4.3.1 Asymptotic analysis

As expected, the equations are $1^{\text{st}}$ and $2^{\text{nd}}$ order differential equations in $r$. To specify the solution uniquely, we need to supplement the equations with a set of boundary conditions. Physically, this corresponds to selecting the normalizable solution that is regular everywhere outside of the black hole singularity. The homogeneous modes of the above equations can be found immediately:

$$\begin{aligned}
h_0^{(n)} &= n_1 + \frac{m_1}{r^3} \\
k_0^{(n)} &= b_1 r + \left(\frac{1}{2r^3}m_2 - 2n_1 r^4\right) \\
j_0^{(n)} &= b_2 + n_2 r^3 \\
\alpha_0^{(n)} &= n_3 + d_1 \log\left(1-\frac{1}{r^3}\right)
\end{aligned} \tag{4.18}$$

We discuss boundary conditions in each of the sectors individually.

**Scalar.** In the expressions for order $n$ contribution to the metric (4.12) and (4.16), $h(r)$ multiplies $\left(2\,dt\,dr - r^2\,dx^2\right)$, which have the potential to perturb the asymptotically flat $g^{(0)}$ if $h$ grows as a constant or larger with $r \to \infty$. To ensure normalizability, we must therefore impose that $h$ grows slower than a constant, which in turn implies that $S_h$ must grow no faster than $\frac{1}{r^3}$. An $\frac{1}{r^2}$ piece in $S_h$ introduces not only a constant mode but also a $\log(r)$ mode which cannot be canceled against the homogeneous modes. If $S_h$ is well-behaved, then we are forced to set $n_1 = 0$.

The other homogeneous mode, $\frac{1}{r^3}$, is pure gauge, which can be removed by redefining $r \to r + \frac{m_1}{r^2}$, which is seen to preserve our gauge choice. As no $\frac{1}{r^3}$ modes arise if $S_h$ grows no faster than $\frac{1}{r^3}$, we can set $m_1 = 0$.

The function $k(r)$ multiplies $\frac{1}{r^2}\,dt^2$, and so it becomes non-renormalizable if $k(r)$ grows as $r^4$ or faster. This in turn requires that $S_k$ grow no faster than $r$. No additional con-

straints are imposed on $S_h$, which enters the differential equation for $k$ through $h$. The $b_1 r$ homogeneous mode gives rise to a $\frac{b_1}{r}\,\mathrm{d}t^2$ term, which is identical in form to the $\frac{1}{b^3 r}\,dt^2$ term in $g^{(0)}$ from $r^2 f(br)\mathrm{d}t^2 = \left(r^2 - \frac{1}{b^3 r}\right)\mathrm{d}t^2$. It can therefore be removed by a redefinition of the field variable $b$. No $r$ modes are generated from sources.

**Vector.** The vector function $j(r)$ multiplies $\frac{1}{r}\,\mathrm{d}x\,\mathrm{d}t$ and so becomes non-renormalizable when $j$ grows as $r^3$ or higher. Terms in $S_j$ that grow as $r$ or faster give rise to terms $r^4$ or higher. A constant term in $S_j$ generates a $r^3$ term which can be canceled against the homogeneous mode $n_2$. No sources we will consider have a constant piece, so we are forced to set $n_2 = 0$.

The other homogeneous mode, $b_2$, can be removed by redefinition of $b$ by the same argument as the $b_1\, r$ mode of $k$. Since we impose $u_\mu T^{\mu\nu} = 0$, we are forced to set $b_2 = 0$. No terms in $S_j$ give rise to constant modes.

**Traceless symmetric tensor.** The tensor function $\alpha(r)$ multiplies $r^2\,\mathrm{d}x^i\,\mathrm{d}x^j$ which becomes non-renormalizable when $\alpha$ grows as a constant or faster. A $r^2$ term in $S_\alpha$ generates a non-renormalizable $\log r$ term that cannot be canceled against the homogeneous modes. All terms with $r^n$ for $n < 2$ generate constant modes, so that the homogeneous $n_3$ has to be fine-tuned to remove them. Additionally, all powers of $r$ generate a $\log(1-r)$ mode, which is divergent at the horizon and has to be canceled by fine-tuning of $d_1$.

### 4.3.2 Results

The analysis of the source terms has been carried out to second order. The various derivatives of $u$ appearing in the resulting expressions can be grouped and covariantized with respect to contractions of $u$ and its derivatives. To aid in the pattern-recognition analysis, it is useful to enumerate all possible scalar, vector and tensor expressions at a given order, together with their local frame form, which we construct below for reference. To this end, we first define the fluid material derivative:

$$\mathcal{D} \equiv u^\alpha \partial_\alpha \tag{4.19}$$

Furthermore, we observe that in order to satisfy our gauge condition 4.13, we only need to consider, in addition to scalars, $u$-orthogonal vectors and $u$-orthogonal traceless symmetric tensors.

The only possibilities at 1$^{\text{st}}$ order are:

$$\begin{aligned}
\mathcal{S}^{(1)} &= \partial_\alpha u^\alpha && \sim \partial_i \beta_i \\
\mathcal{V}^{(1)\mu} &= \mathcal{D} u_\mu && \sim \partial_t \beta_i \\
\sigma_{\mu\nu} \equiv \mathcal{T}^{(1)}_{\mu\nu} &= \Pi_{\mu\nu}{}^{\alpha\beta}\, \partial_\alpha u_\beta && \sim \frac{1}{2}\left(\partial_i \beta_j + \partial_j \beta_i\right) - \frac{1}{4}\,\delta_{ij}\,\partial_k \beta_k
\end{aligned}$$

At second order, we find more possibilities [14]:

$$
\begin{aligned}
\mathcal{S}_3^{(2)} &= u^\alpha \partial_\alpha \partial_\beta u^\beta - \mathcal{D}u^\mu \, \mathcal{D}u_\mu \\
\mathcal{S}_4^{(2)} &= \mathcal{D}u^\alpha \, \mathcal{D}u_\alpha \\
\mathcal{S}_5^{(2)} &= (\partial_\alpha u^\alpha)^2 \\
\mathcal{S}_6^{(2)} &= \left(\epsilon^{\alpha\beta\gamma} \, u_\alpha \, \partial_\beta u_\gamma\right)^2 \\
\mathcal{S}_7^{(2)} &= \sigma^{\alpha\beta} \, \sigma_{\alpha\beta} \\
\mathcal{V}_{3\mu}^{(2)} &= P_\mu{}^\alpha \left(\partial_\alpha \partial_\beta u^\beta - \mathcal{D}u_\beta \, \partial_\alpha u^\beta\right) \\
\mathcal{V}_{4\mu}^{(2)} &= P_\mu{}^\alpha \, P^{\beta\gamma} \, \partial_\beta \partial_\gamma u_\alpha \\
\mathcal{V}_{5\mu}^{(2)} &= P_\mu{}^\alpha \, \partial_\beta u^\beta \, \mathcal{D}u_\alpha \\
\mathcal{V}_{6\mu}^{(2)} &= P_\mu{}^\alpha \, \mathcal{D}u_\beta \, \partial_\alpha u^\beta \\
\mathcal{T}_{2\mu\nu}^{(2)} &= \Pi_{\mu\nu}{}^{\alpha\beta} \, (\mathcal{D}\partial_\alpha u_\beta) \\
\mathcal{T}_{3\mu\nu}^{(2)} &= \Pi_{\mu\nu}{}^{\alpha\beta} \, (\mathcal{D}u_\alpha \, \mathcal{D}u_\beta) \\
\mathcal{T}_{4\mu\nu}^{(2)} &= \Pi_{\mu\nu}{}^{\alpha\beta} \, (\partial_\gamma u_\alpha \, \partial^\gamma u_\beta + \mathcal{D}u_\alpha \, \mathcal{D}u_\beta) \\
\mathcal{T}_{5\mu\nu}^{(2)} &= \Pi_{\mu\nu}{}^{\alpha\beta} \, (\partial_\alpha u_\gamma \partial_\beta u^\gamma)
\end{aligned}
$$

Finally, the 1st order source terms are given by:[2]

$$
\begin{aligned}
S_h^{(1)}(r) &= 0 \\
S_k^{(1)}(r) &= -4r \, \mathcal{S} \\
S_j^{(1)}(r) &= -\frac{1}{r} \mathcal{V} \\
S_\alpha^{(1)}(r) &= 2r \, \mathcal{T}
\end{aligned}
\tag{4.20}
$$

All of the first order sources satisfy power scaling conditions at $r \to \infty$ imposed by normalizability and regularity. We can therefore integrate equations (4.17) for $h$, $k$, $j$ and $\alpha$ and set boundary conditions in accordance to the discussion of the previous section. The results are:

$$
\begin{aligned}
h(r) &= 0 \\
k(r) &= r^3 \, \mathcal{S} \\
j(r) &= r^2 \, \mathcal{V} \\
\alpha(r) &= 2 \, F(r) \, \mathcal{T}
\end{aligned}
\tag{4.21}
$$

[2]Indices "(1)" and tensor indices suppressed for clarity.

where $F(r)$ is defined as:

$$\begin{aligned} F(r) &= -\int_{\infty}^{r} dr\, \tfrac{1+r}{r(1+r+r^2)} = -\tfrac{\sqrt{3}}{3}\tan^{-1}\left(\tfrac{\sqrt{3}}{3}(2r+1)\right) + \tfrac{1}{2}\log\left(\tfrac{1+r+r^2}{r^2}\right) + \tfrac{\sqrt{3}\pi}{6} \\ &\approx \tfrac{1}{r} - \tfrac{1}{3r^3} + \tfrac{1}{4r^4} + \mathcal{O}\left(\tfrac{1}{r^5}\right) \end{aligned} \tag{4.22}$$

The second order sources are considerably more complicated:[3]

$$\begin{aligned} S_h^{(2)}(r) &= -\tfrac{1}{2r^4}\,\mathcal{S}_6 + F_1(r)\,\mathcal{S}_7 \\ S_k^{(2)}(r) &= 2\,\mathcal{S}_3 + \tfrac{1}{2}\,\mathcal{S}_5 - \tfrac{1+4r^3}{2r^3}\,\mathcal{S}_6 + F_2(r)\,\mathcal{S}_7 \\ S_j^{(2)}(r) &= \tfrac{1}{2r^2}\,\mathcal{V}_3 - \tfrac{1}{2r^2(1+r+r^2)}\,\mathcal{V}_4 + \tfrac{-1+r+r^2}{2r^2(1+r+r^2)}\,(\mathcal{V}_5 - \mathcal{V}_6) \\ S_\alpha^{(2)}(r) &= F_3(r)\,(\mathcal{T}_2 + \mathcal{T}_3) + F_4(r)\,\mathcal{T}_4 + F_5(r)\,\mathcal{T}_5 \end{aligned} \tag{4.23}$$

Where the various $r$-dependent functions are defined as follows:

$$\begin{aligned} F_1(r) &= \tfrac{2(1+2r)}{r^2(1+r+r^2)^2}\,F(r) - \tfrac{(1+r)^2}{r^2(1+r+r^2)^2} && \approx -\tfrac{1}{r^4} + \tfrac{6}{r^6} + \mathcal{O}\left(\tfrac{1}{r^7}\right) \\ F_2(r) &= 2\,\tfrac{1+r-4r^3-4r^4}{r(1+r+r^2)}\,F(r) + \tfrac{-1+2r+4r^2+4r^3}{r+r^2+r^3} && \approx -4 + \tfrac{26}{3r^2} + \mathcal{O}\left(\tfrac{1}{r^3}\right) \\ F_3(r) &= 2r\,F(r) - \tfrac{2r(1+r)}{1+r+r^2} && \approx \tfrac{4}{3r^2} - \tfrac{3}{2r^3} + \mathcal{O}\left(\tfrac{1}{r^5}\right) \\ F_4(r) &= -\tfrac{r}{2}\,F(r) - \tfrac{1}{2(1+r+r^2)} && \approx -\tfrac{1}{2} - \tfrac{1}{3r^2} + \mathcal{O}\left(\tfrac{1}{r^3}\right) \\ F_5(r) &= \tfrac{3}{2}\,r\,F(r) + \tfrac{1-2r-2r^2}{2(1+r+r^2)} && \approx \tfrac{1}{2} + \tfrac{1}{r^2} + \mathcal{O}\left(\tfrac{1}{r^3}\right) \end{aligned}$$

All of the second order terms follow the prescribed power scaling as $r \to \infty$, so $h$, $k$, $j$ and $\alpha^{(2)}$ can be obtained by integrating their respective equations (4.17) and setting boundary conditions. Not all of the $r$ functions are exactly (or easily) integrable. For those that are, we present a closed form solution below. Non-integrable functions are presented as a series expansion in $\frac{1}{r}$ at relevant orders. The precise form can be obtained by integrating

[3]Indices "(2)" and tensor indices suppressed for clarity.

numerically equations in (4.17) for the relevant source terms.

$$
\begin{aligned}
h^{(2)} &= \tfrac{1}{4r^2}\,\mathcal{S}_6 + \Big[\tfrac{1}{2r^2} + \mathcal{O}\left(r^{-4}\right)\Big]\mathcal{S}_7 \\
k^{(2)} &= -r^2\,\mathcal{S}_3 - \tfrac{r^2}{4}\,\mathcal{S}_5 + \Big[r^2 - \tfrac{1}{8r}\Big]\mathcal{S}_6 + \Big[2\,r^2 + \mathcal{O}\left(r^0\right)\Big]\mathcal{S}_7 \\
j^{(2)} &= -\tfrac{r}{2}\,\mathcal{V}_3 + \Big[-\tfrac{r^2}{3} + \tfrac{r}{6} + \left(1 - r^3\right)\left(\tfrac{\pi}{9\sqrt{3}} - \tfrac{2}{3\sqrt{3}}\tan^{-1}\left(\tfrac{2+r}{\sqrt{3}r}\right)\right)\Big]\mathcal{V}_4 \\
&\quad + \Big[-\tfrac{2r^2}{3} - \tfrac{r}{6} + 2\left(1 - r^3\right)\left(\tfrac{\pi}{9\sqrt{3}} - \tfrac{2}{3\sqrt{3}}\tan^{-1}\left(\tfrac{2+r}{\sqrt{3}r}\right)\right)\Big]\left(\mathcal{V}_5 - \mathcal{V}_6\right) \\
&\approx -\tfrac{r}{2}\,\mathcal{V}_3 - \Big[\tfrac{1}{4r} + \mathcal{O}\left(r^{-2}\right)\Big]\mathcal{V}_4 - \Big[\tfrac{r}{2} + \tfrac{1}{2r} + \mathcal{O}\left(r^{-2}\right)\Big]\left(\mathcal{V}_5 - \mathcal{V}_6\right) \\
\alpha^{(2)} &\approx \Big[\left(\tfrac{2}{3} + A\right)\tfrac{1}{r^3} + \mathcal{O}\left(r^{-4}\right)\Big]\left(\mathcal{T}_2 + \mathcal{T}_3\right) + \Big[-\tfrac{1}{2r^2} + \tfrac{1}{4}\left(\tfrac{2}{3} - A\right)\tfrac{1}{r^3} + \mathcal{O}\left(r^{-4}\right)\Big]\mathcal{T}_4 \\
&\quad + \Big[\tfrac{1}{2r^2} + \tfrac{3}{4}\left(\tfrac{2}{9} + A\right)\tfrac{1}{r^3} + \mathcal{O}\left(r^{-4}\right)\Big]\mathcal{T}_5 \\
&\approx \tfrac{1}{2r^2}\left(\mathcal{T}_5 - \mathcal{T}_4\right) + \tfrac{2}{3r^3}\left[\tfrac{1}{2}A\left(\mathcal{T}_2 + \mathcal{T}_3 + \tfrac{1}{4}\mathcal{T}_4 + \tfrac{1}{4}\mathcal{T}_5\right) + (A-2)\left(\tfrac{1}{4}\mathcal{T}_5 - \tfrac{1}{4}\mathcal{T}_4\right)\right] + \mathcal{O}\left(r^{-4}\right)
\end{aligned}
\tag{4.24}
$$

where

$$
A = \tfrac{\pi}{3\sqrt{3}} - \log 3 + 2 \tag{4.25}
$$

Tensors $\mathcal{T}$ appearing in the expression for $\alpha$ have been organized in a very peculiar fashion for the reason that those linear combination collapse into simple tensorial expressions [14]:

$$
\begin{aligned}
\Sigma_1^{\mu\nu} = \mathcal{T}_2 + \mathcal{T}_3 + \tfrac{1}{4}\mathcal{T}_4 + \tfrac{1}{4}\mathcal{T}_5 &= \Pi^{\mu\nu}{}_{\alpha\beta}\left(\mathcal{D}\sigma^{\alpha\beta} + \tfrac{1}{2}\sigma^{\alpha\beta}\,\partial_\gamma u^\gamma\right) \\
\Sigma_2^{\mu\nu} = \tfrac{1}{4}\mathcal{T}_5 - \tfrac{1}{4}\mathcal{T}_4 &= \Pi^{\mu\nu}{}_{\alpha\beta}\left(\sigma_\gamma{}^\alpha\,\omega^{\beta\gamma}\right)
\end{aligned}
\tag{4.26}
$$

with $\omega^{\mu\nu}$ being the completely anti-symmetric relativistic $u$-orthogonal vorticity defined as:

$$
\omega^{\mu\nu} = \tfrac{1}{2}\,P^\mu{}_\alpha\,P^\nu{}_\beta\left(\partial^\alpha u^\beta - \partial^\beta u^\alpha\right) \tag{4.27}
$$

Let us briefly summarize what has been done. At orders $n = 1$ and $n = 2$ we have expanded the known order $n-1$ solution around $x^\mu$ up to $n^{\text{th}}$ order. The $x^\mu$ dependence of the order $n-1$ metric had only been through $u$ and $b$ functions of $x^\mu$, so in the process we have produced a great number of derivatives of $u$. We have also boosted to a local coordinate frame where $u = (1,0,0)$ while simultaneously rescaling the $r$ coordinate so that $b = 3/4\pi T = 1$. We have then run the Einstein machinery, collected results, which we then covariantized with respect to $u$, effectively undoing the choice of the local coordinate frame. We have yet to generalize the solution with respect to $T$ by rescaling the $r$ coordinate. This is most easily accomplished using dimensional analysis.

This completes the solution of the out-of-equilibrium black hole at $2^{\text{nd}}$ order in derivatives of the perturbation. The black hole metric is given by summing the first 3 terms in the derivative expansion with the $r$-dependent functions given by eqs. (4.21) and (4.24).

We note that most of our results agree with their original presentation in [14], with a

minor, but significant exception. We find that the functional forms of $S_k^{(2)}$ and thus also $k^{(2)}$ differ from those derived in [14]. As the Brown-York tensor is only sensitive to the traceless symmetric sector of the metric, this discrepancy does not influence the fluid dynamics.

### 4.3.3 Hydrodynamic constraints

We now return to the dynamical equations. As advertised earlier, we find that the dynamical equations at any order $n$ are the conservation equations of the Brown-York stress energy tensor built out of the order $n-1$ metric. The structure of the equations as uncovered in the perturbation calculation is best described in terms of induction. Performing the calculation at order $n=1$, we find conservation equations of the $0^{\text{th}}$ order stress energy tensor. At any order $n>1$ we find two sets of equations: one set constitutes precisely the equations of conservation of the $n-2$ order stress energy tensor *expanded* around $x^\mu = 0$, so that the number derivatives of $u$ matches the order $n$ of the calculation. This guarantees that the previously found conservation equations of the $n-2$ order stress energy tensor remain to hold covariantly at all orders in perturbation theory. In addition, we also find new conservation equations for the $n-1$ contribution of the tensor.

Summarizing, a metric constrained in a manner described in the previous section is a perturbative solution to Einstein field equations at order $n$ if $u$ and $T$ obey:

$$\partial_\mu \left( \sum_{n=0}^{n-1} T^{\mu\nu}_{(i)} \right) = 0 \tag{4.28}$$

For completeness, the contributions to the Brown-York stress energy tensor computed at orders 0, 1, and 2 are:

$$\begin{aligned} T^{\mu\nu}_{(0)} &= \frac{1}{2}\left(\frac{4\pi T}{3}\right)^3 (\eta^{\mu\nu} + 3\, u^\mu\, u^\nu) \\ T^{\mu\nu}_{(1)} &= -\left(\frac{4\pi T}{3}\right)^2 \sigma^{\mu\nu} \\ T^{\mu\nu}_{(2)} &= \left(\frac{4\pi T}{3}\right)\left(\frac{A}{2}\Sigma_1^{\mu\nu} + (A-2)\Sigma_2^{\mu\nu}\right) \end{aligned} \tag{4.29}$$

## 4.4 Numerical calculation

Analytical expressions that relate the dynamics of an out-of-equilibrium black hole and relativistic conformal fluid provide us with a great advantage. Einstein equations are second order non-linear differential equations with diffeomorphism redundancy, whose solution requires imposing of non-trivial normalizability conditions, and whose domain is a $n = 3 + 1$ dimensional manifold. Solving the equations using numerical methods, while possible [23], is complicated. The fluid equations, on the other hand, have trivial boundary conditions and are relatively straightforward. In addition, the spatial domain of the hydrodynamical system is only 2-dimensional. Using the derived duality, we can construct dynamical solutions to Einstein gravity without solving Einstein field equations directly, but instead building the solution in a perturbative expansion using a solution to the considerably simpler hydro system.

In order for the perturbative solution to hold at $2^{\text{nd}}$ order, it is required that we solve the hydrodynamics of the $1^{\text{st}}$ order stress-energy tensor. This poses a problem, however, as it is well known that first order hydrodynamics develops singular wave fronts [4], and is thus unsuitable for numerical simulations. Nevertheless, assuming that the hydrodynamic approximation holds (cf. Sec 2), we are free to add a second order term of our choice at a cost of introducing errors no greater than second order. Such errors do not invalidate the perturbative construction of the metric and are therefore acceptable.

An identical numerical simulation of the $2 + 1$-dimensional hydrodynamical system has been carried out independently by A. Adams and P. Chesler in 2012 and the results were found in excellent agreement. In addition, in [23] authors pursue a numerical simulation in a reverse order: having solved Einstein gravity on $AdS_4$ they numerically extract the stress-energy tensor of the dual flow.

### 4.4.1 Setup

We solve second order relativistic $2+1$ fluid dynamics by numerically integrating dynamical equations that arise as conservation equations of the $2^{\text{nd}}$ order Brown-York tensor dual to an out-of-equilibrium black hole in $3 + 1$ dimension. The system of coupled differential equations of order 3 in $u$ and order 1 in $T$ is converted into a system of equations of order 1. The simulation is carried out with an explicit Runge-Kutta (4,5) method with a variable time step on a regularly spaced 2-dimensional grid with periodic boundary conditions. Spatial derivatives are computed using the Fourier spectral method [8]. The number of collocation points is chosen specific to initial conditions or purposes of the simulation and will be discussed alongside presentation of the results. For convenience, we rescale the fluid temperature in all what follows as:

$$\mathfrak{T} = \frac{4\pi T}{3} \tag{4.30}$$

The black hole geometry is constructed numerically by realizing the order 2 metric con-

structed in the previous section evaluated on the solution of the hydrodynamical system. The metric at each time step is evaluated on a 3-dimensional grid that is the outer product of the regular square periodic grid used for hydro simulation, and a radial direction evaluated on Chebyshev collocation points. In this way, spatial derivatives along the transverse coordinates $x^\mu$ are computed using the Fourier spectral method, while derivatives along the radial coordinate using the Chebyshev spectral method[4] [8]. Number of collocation points along the radial dimension that guarantees good error convergence in our application is $N_z = 32$. The radial coordinate is re-parametrized to bring the semi-infinite coordinate range $(r_{\rm H}, \infty)$ to a finite interval $(1/r_{\rm H}, 0)$:

$$r \longrightarrow 1/z \tag{4.31}$$

The radial coordinate domain is $(0, 1/r_{\rm H})$. The time steps are evenly spaced, and time derivatives of $g_{\mu\nu}$ and $\Gamma^\mu_{\nu\sigma}$ used for purposes of calculating of GR tensors are evaluated using an order 5 finite central difference method. To ensure numerical accuracy, the hydrodynamical equations, $g$ and $\Gamma$ are evaluated at a grid that is super-sampled with respect to the desired evaluation points of the GR tensors.

The non-integrable components of radial functions appearing in expression for $g^{(2)}$ (that is: the functions multiplying $\mathcal{S}_7$ in $h^{(2)}$, $\mathcal{S}_7$ in $k^{(2)}$, and $\mathcal{T}_2 + \mathcal{T}_3$, $\mathcal{T}_4$ and $\mathcal{T}_5$ in $\alpha^{(2)}$) are integrated numerically on $z \in (0, 2)$[5]. The $r$ dependence is independent of the transverse coordinates, and so the $r$-functions can be pre-computed ahead of time. $h$ and $k$ are computed using a Runge-Kutta solver (imposing of the boundary conditions is straightforward), while the $\alpha$ terms are computed on a Chebyshev grid through inversion of the Chebyshev derivative matrix to ensure regularity at the horizon. The results are interpolated using spectral methods onto a very dense equispaced grid ($N = 2048$) so that to allow fast linear look-up while producing numerical errors that are sub-leading.

### 4.4.2 Results

We have successfully implemented numerical integration of the second order hydro equations, as well as the numerical metric up to the second order in derivatives of the fluid velocity.

We have verified qualitatively that the fluid dynamics exhibits relativistic features: we observed length contraction watching a relativistic wave packet spread faster in directions transverse to its direction of motion, and time dilation watching the spreading out of a super-relativistic wave packet slow down to a near halt.

[4]We thank Paul Chesler for his prototype implementation of the various Chebyshev spectral methods that has been adapted to our purposes.

[5]Notice that all of $h$, $k$, $j$, $\alpha$ are evaluated on $b/z$, and that $b/r_{\rm H} = 1$, so that we only need to know the functions between the boundary $b/z = 0$ and just beyond the horizon $b/z = 1$ ("just beyond" due to thermal fluctuations in $T \propto \frac{1}{b}$).

**Testing the black hole metric.** We would like to verify that we have correctly solved the GR equations and implemented the solution in accordance to the prescription of Sec. 4.3. Ideally, we would like to quantify how far the metric we have constructed deviates from the true solution and whether the deviation diminishes with the addition of higher order terms. Such computation is, naturally, impossible, for we have no knowledge of the true metric nor higher order contributions beyond order 2. Nevertheless, gravity provides us with other tools at our disposal. The trace of the Einstein tensor should vanish identically on the true solution, so probing how $\operatorname{tr} E$ changes as we add higher order pieces might provide us with enough information to determine whether we are correctly solving the equations. Notice however, that while we expect a power law scaling of errors in the expression of the metric, this is no longer true of the Einstein tensor as it involves various powers of the metric, its inverse, as well as its derivatives.

We conduct the error analysis on two levels: investigate the superficial scaling law of the Einstein trace for a metric constructed at the $0^{\text{th}}$, $1^{\text{st}}$, and $2^{\text{nd}}$ order, and also investigate the scaling law of the error as we vary physical length scales of the theory. There are multiple ways to change the physical scales, guaranteed by the conformal invariance of the fluid dynamics. We could rescale the transverse coordinates while keeping the numerical value of the velocity field constant so that to vary the gradients only. This has the obvious disadvantage of changing the time scale of the simulation, making it harder to compare the results. Alternatively, we could rescale the temperature and achieve the same effect at the cost of changing the position of the black hole apparent horizon.

We observe that both of those operations have an equivalent effect of changing the scale of energy dissipation in the system. Changing the transverse coordinates amounts to scaling up and down the relative size of the wavelengths of velocity variation and the dissipation scale. Similarly, changing the temperature changes the dissipation scale while holding the size of velocity variations fixed, which can be established easiest with dimensional analysis: temperature is the only dimensionful parameter in the theory, and by dimensional analysis $\ell_{\text{dissipation}} \sim 1/T$. For this reason, we expect that the computational effort required to solve the numerical equations at a fixed numerical accuracy go up as we increase temperature.

Lastly, we need to specify what precisely is meant by "comparing traces of $E$". The only covariant way of doing this involves integrating the trace (or its absolute value) over the manifold:

$$\varepsilon'(\mathfrak{T}) = \int_{1/\mathfrak{T}}^{0} dr \int dx^{\mu} \sqrt{-\det g} \left| \operatorname{tr} E \right| \tag{4.32}$$

However, as $\sqrt{-\det g} \sim \frac{1}{z^4}$ and $\operatorname{tr} E \sim z$ near the boundary, the above integral diverges, and in particular cannot be evaluated numerically. Alternatively, we could compare $\operatorname{tr} E$ at a particular $z$ slice. The only distinguished point is naturally $z = 1/\mathfrak{T}$, so we define:

$$\varepsilon(\mathfrak{T}) = \int dx^{\mu} \left| \operatorname{tr} E \right|_{z=1/\mathfrak{T}} \tag{4.33}$$

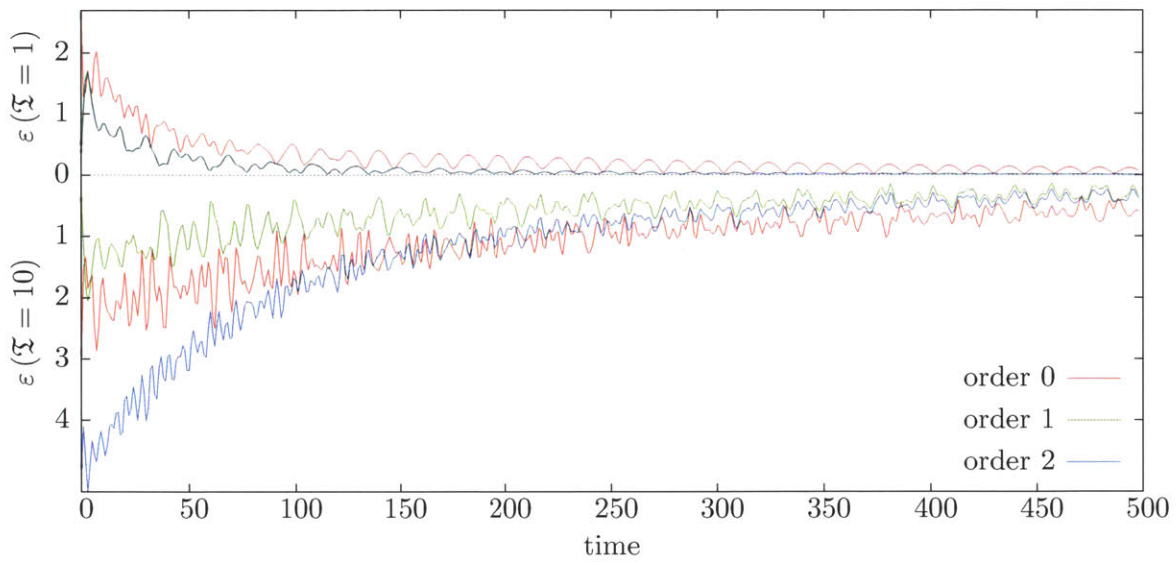


Figure 4-1: Errors $\varepsilon$ for $\mathfrak{T}_0 = 1$ (upper half) and $\mathfrak{T}_0 = 10$ (lower half, flipped vertically) calculated for $g_{\mu\nu}$ computed to $0^{\text{th}}$, $1^{\text{st}}$, and $2^{\text{nd}}$ orders. Errors at $1^{\text{st}}$ and $2^{\text{nd}}$ orders at $\mathfrak{T}_0 = 1$ agree exactly. Fluid velocity initial conditions given as random superposition of 1000 sinusoidal modes of wavelengths between $L$ and $L/5$, normalized to $\max|u| = 0.1$.

We simulate the relativistic hydrodynamics on a grid with $N_x = N_y = 32$ collocation points of physical length $L = 100$ for $\mathfrak{T} = 1$, $\mathfrak{T} = 10$, and $\mathfrak{T} = 100$, corresponding to three different regimes: dissipation scale comparable to the size of perturbations, intermediate scale, and dissipation scale smaller than the size of the perturbation. The initial conditions are a constant $\mathfrak{T}$ and a random perturbation of $u$: superposition of 1000 sinusoidal modes of random wavelengths between $L$ and $L/5$, random polarizations and phase shifts, normalized so that $\left|\max u\right| = 0.1$. The results are shown on Fig. 4-1.

First of all, we observe the errors diminish in size as time goes on, a fact which agrees qualitatively with high frequency modes being lost to dissipation. Furthermore, errors diminish in size between the $0^{\text{th}}$ and $1^{\text{st}}$ order, confirming that the effect of including of the $1^{\text{st}}$ order piece is indeed to improve $g_{\mu\nu}$ as a solution to Einstein equations. The errors of the second order calculation are less conclusive. In particular, it appears that increasing the temperature for otherwise identical initial conditions causes the $2^{\text{nd}}$ order error to grow. This is very disconcerting, and it very strongly suggests a mistake in the second order code – it is very plausible that an extra factor of $z$ or $T$ multiplying any part of any contribution to the second order metric would effectively increase the error.

Summing up, analysis of errors quantified by the vanishing of $\operatorname{tr} E$ verifies that the first order metric is an improvement over the naive $0^{\text{th}}$ order black hole. The results at second order do not support the validity of the metric perturbation expansion, possibly due to problems in the code.

**Turbulence.** Motivated by the long-standing question of the mathematical description of turbulence, let us now investigate whether the fluid dual to the out-of-equilibrium black hole is capable of supporting turbulent phenomena. To this end, we simulate the flow of linear streams gushing past each other with a small random perturbation. The simulation is computed on a regularly spaced periodic grid with $N_x = N_y = 128$ collocation points. The comparatively higher resolution is necessary to resolve small-scale features that appear at the onset of turbulence. The resolution is high enough to accurately describe only a few turbulent vortices, so the results should be treated as a quick-and-simple test-of-concept.

A similar computation has been carried out for a $2+1$ relativistic conformal $0^{\text{th}}$ order (i.e. ideal) fluid on a sphere in [22]. The numerical results of [22] do exhibit turbulent behavior as well.

The results for $\mathfrak{T} = 250$ and $\mathfrak{T} = 500$ are displayed on Fig. 4-3 and 4-4, respectively. We find a spectacular formation of turbulent vortices immediately after momentum of the disrupted streams begins to flow sideways. As soon as turbulent behavior displaces energy into higher frequency modes, the two simulations begin to differ in agreement with the difference of their dissipation scales. Higher frequency modes are dissipated more rapidly for $\mathfrak{T} = 250$ in comparison with $\mathfrak{T} = 500$, which is manifested in smoother shapes and eventual dissipation of the vortices.

It is well-known that turbulent non-relativistic systems exhibit Kolmogorov $k^{-5/3}$ scaling of the energy power spectrum $\mathcal{H}(t,k)$ that measures kinetic energy per momentum mode, defined for a two-dimensional fluid as:

$$= \frac{\partial}{\partial k} \int_{|k'|<k} d^2k' \, \bar{u}(t,k)^i \, \bar{u}(t,k)_i \tag{4.34}$$

where $\bar{u}$ are the Fourier modes of the fluid velocity. We compute the *relativistic* kinetic energy power spectrum and find out that indeed the fluid exhibits Kolmogorov scaling as soon as turbulence ensues. Fig. 4-2 shows the power spectra for $\mathfrak{T} = 10$ at two different times: immediately before turbulence develops ($t = 800$), and at a time when turbulence is visually most pronounced ($t = 2200$).

We find that the relativistic fluid with smaller dissipation scale ($\mathfrak{T} = 500$) exhibits consistent Kolmogorov scaling in its turbulent regime. The fluid with $\mathfrak{T} = 250$ is less consistent: the $k^{-5/3}$ scaling law switches on and off throughout the simulation. In addition, we observe that the $k^{-5/3}$ region "sheds" ripples down towards the higher frequency end of the spectrum, confirming that the inverse energy cascade of a $2+1$ dimensional fluid. One should remember that the Kolmogorov scaling behavior has been observed in a small-scale simulation with only two turbulent vortices. In order to extract statistically meaningful results one should carry out an analogous analysis on a grid dense enough to allow for multiple vortices as well as interactions between them.

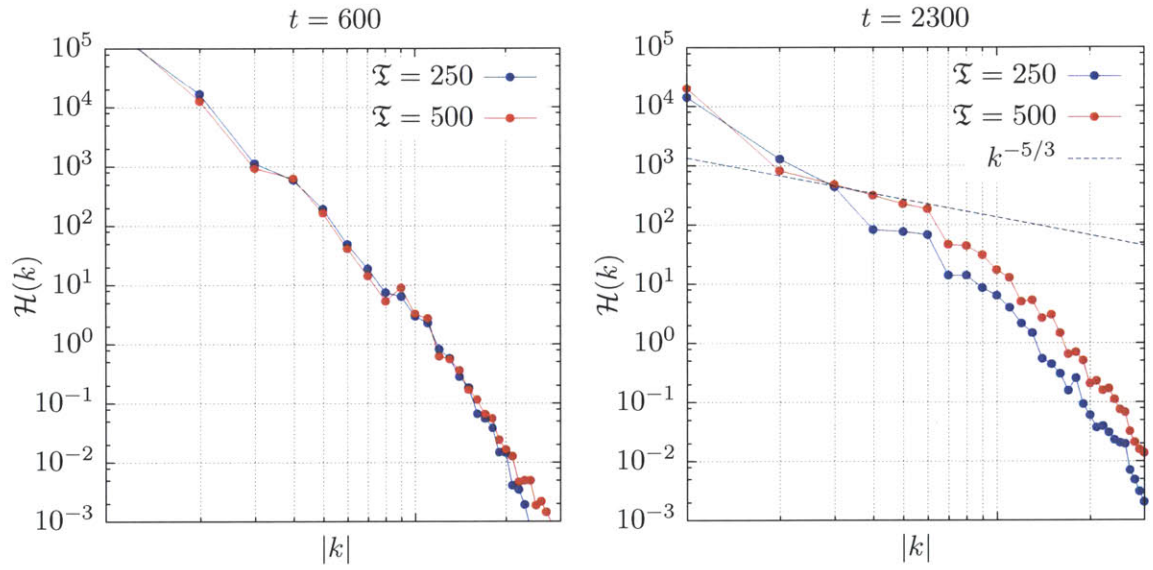


Figure 4-2: Power spectrum of relativistic turbulent fluid flow for $\mathfrak{T} = 250$ and $\mathfrak{T} = 500$ plotted at two points in time: $t = 600$ (laminar) and $t = 2300$ (turbulent). The $\mathfrak{T} = 500$ flow exhibits Kolmogorov scaling in its turbulent regime.

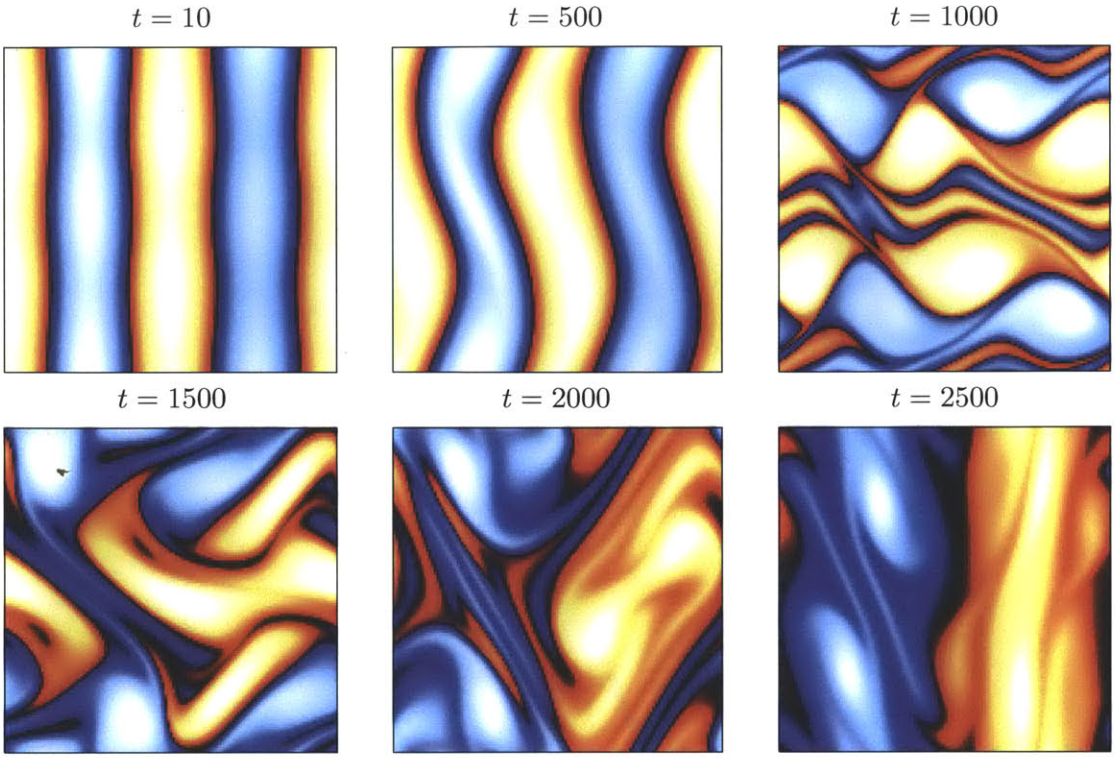


Figure 4-3: Vorticity of fluid evolution for $\mathfrak{T} = 250$, $L = 40$. Initial conditions of four streams gushing past one another are perturbed slightly. Perturbations disrupt the regular flow giving rise to turbulence. High-frequency modes dissipate.

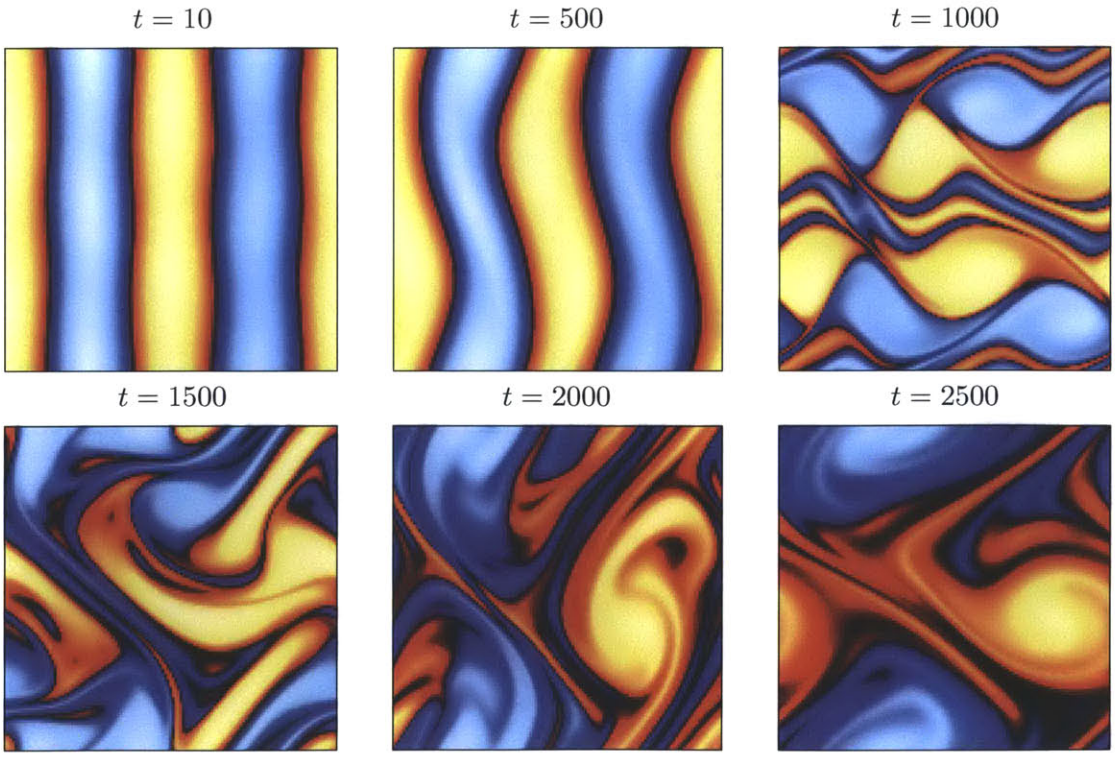


Figure 4-4: Vorticity of fluid evolution for $\mathfrak{T} = 500$, $L = 40$, same initial conditions. Shorter dissipation scale $\sim 1/\mathfrak{T}$ causes slower dissipation of the turbulent flow.

# Bibliography


[1] C. W. Misner, K. S. Thorne, J. A. Wheeler, "*Gravitation*", W. H. Freeman and Company (1932).

[2] L. D. Landau, E. M. Lifshitz, "*Fluid Mechanics. Course of Theoretical Physics, Vol. 6*", Pergamon Press (1959).

[3] S. W. Hawking, G. F. R. Ellis, "*The large scale structure of space-time*", Cambridge University Press (1973).

[4] W. Israel, J. Stewart, "*Transient Relativistic Thermodynamics and Kinetic Theory*", Ann. of Phys. **118**, (1978).

[5] R. M. Wald, "*General Relativity*", The University of Chicago Press (1984).

[6] J. Podolsky, "*Lorentz boosts in de Sitter and anti-de Sitter space-times*", Czechoslovak Journal of Physics, **43**, pp1173-1176, (1993).

[7] J. M. Maldacena, "*The Large N Limit of Superconformal field theories and supergravity*", Adv. Theor. Math. Phys. 2, (1998).

[8] L. Trefethen, "*Spectral Methods in Matlab*", SIAM, (2001).

[9] S. Carroll, "*Spacetime and Geometry. An Introduction to General Relativity*", Addison Wesley (2004).

[10] U. Moschella, "*The de Sitter and anti-de Sitter Sightseeing Tour*", (2005).

[11] N. Anderson, "*Relativistic fluid dynamics: physics for many different scales*", Living Rev. Rel. 10 (2006), arXiv:gr-qc,0605010v2.

[12] M. Kardar, "*Statistical Physics of Particles*", Cambridge University Press (2007).

[13] S. Bhattacharyyaa, V. E. Hubeny, S. Minwalla, M. Rangamani, "*Nonlinear Fluid Dynamics from Gravity*", JHEP 0802:045 (2008), arXiv:0712.2456v4.

[14] M. Van Raamsdonk, "*Black Hole Dynamics From Atmospheric Science*", JHEP 0805:106 (2008), arXiv:0802.3224v3.

[15] S. Bhattacharyyaa, R. Loganayagam, I. Mandal, S. Minwalla, A. Sharma, "*Conformal Nonlinear Fluid Dynamics from Gravity in Arbitrary Dimensions*", JHEP 0812:116, arXiv:0809.4272v2.

[16] M. Rangamani, "*Gravity & Hydrodynamics: Lectures on the fluid-gravity correspondence*", Class. Quant. Grav. 26 (2009), arXiv:0905.4352v3.

[17] V. Balasubramanian, P. Kraus, "*A Stress Tensor For Anti-de Sitter Gravity*", Commun. Math. Phys. 208, (2009), arXiv:hep-th,9902121vt.

[18] J. Casalderrey-Solana, H. Liu, D. Mateos, K. Rajagopal, U. A. Wiedemann, "*Gauge/String Duality, Hot QCD and Heavy Ion Collisions*", arXiv:1101.0618v2 (2011)

[19] V. E. Hubeny, S. Minwalla, M. Rangamani, "*The fluid,gravity correspondence*", Black Holes in Higher Dimensions, Cambridge University Press (tbp), arXiv:1107.5780v1 (2011).

[20] N. Tetradis, "*Holographic horizons*", arXiv:1109.2335v1 (2011).

[21] A. W. Adams, L. D. Carr, T. Schaefer, P. Steinberg, J. E. Thomas, "*Focus on Strongly Correlated Quantum Fluids: from Ultracold Quantum Gases to QCD Plasmas*", New J. Phys. 14 (2012).

[22] F. Carrasco, L. Lehner, R. Myers, O. Reula, A. Singh, "*Turbulent flows for relativistic conformal fluids in 2+1 dimensions*", arXiv:1210.6702 (2012).

[23] A. W. Adams, P. M. Chesler, H. Liu, "*Holographic turbulence*", to appear in 2013.